經濟部

出國報告(出國類別：考察)

# 近海水文觀測與資料分析技術研習

# Study on the Technology of Coastal Ocean Observation and Data Analysis

服務機關：經濟部水利署
出國人職稱：副工程司
姓　名：王仲豪
出國地點：德國
出國期間：98年10月19日至98年11月2日
報告日期：98 年 12 月 21 日

出國報告(出國類別：考察)

# 近海水文觀測與資料分析技術研習

# Study on the Technology of Coastal Ocean Observation and Data Analysis

服務機關：經濟部水利署
出國人職稱：副工程司
姓 名：王仲豪
出國地點：德國
出國期間：98年10月19日至98年11月2日
報告日期：98 年 12 月 21 日

# 提要表

| | | | | | | |
|---|---|---|---|---|---|---|
| **系統識別號：** | C09804134 | | | | | |
| **計畫名稱：** | 經濟部 98 年度台德技術合作人員訓練計畫 | | | | | |
| **報告名稱：** | 近海水文觀測與資料分析技術研習 | | | | | |
| **計畫主辦機關：** | 經濟部水利署 | | | | | |
| **出國人員：** | 姓名 | 服務機關 | 服務單位 | 職稱 | 官職等 | E-MAIL 信箱 |
| | 王仲豪 | 經濟部水利署 | 水文技術組 | 副工程司 | 聯絡人<br>薦任(派) | a610130@wra.gov.tw |
| **前往地區：** | 德國 | | | | | |
| **參訪機關：** | GKSS(Gesellschaft für Kernenergieverwertung in Schiffbau und Schifffahrt)研究中心 | | | | | |
| **出國類別：** | 考察 | | | | | |
| **出國期間：** | 民國 98 年 10 月 19 日 至 民國 98 年 11 月 02 日 | | | | | |
| **報告日期：** | 民國 98 年 12 月 21 日 | | | | | |
| **關鍵詞：** | 近海水文觀測，GKSS 研究中心，雷達遙測，波浪，海流 | | | | | |
| **報告書頁數：** | 71 頁 | | | | | |
| **報告內容摘要：** | 本次赴德國 GKSS 研究中心進行 15 天之「近海水文觀測與資料分析技術研習」，係獲 98 年度經濟部國際合作處台德技術合作人員訓練計畫核定。研習內容有雷達遙測原理、雷達遙測技術之進展、雷達遙測應用於海洋現象觀測、GKSS 中心研發之雷達遙測資料分析數值模式-Disc 介紹、現地觀測站作業觀摩與討論及現地觀測站之管理與維護方式之研習等。在為期 15 天之研習時間，吸收 GKSS 研究中心應用雷達技術進行近海水文觀測作業之原理，以及雷達觀測資料之核心分析技術及模式，並藉由觀摩 4 處岸基雷達觀測站及其維護管理作業，獲得關於岸基雷達系統更為詳細之運作流程。本次研習已初布獲得可茲水利署於未來發展非接觸式近海水文觀測技術之參考，以及我國與德國海岸工程研究機構，未來進一步進行國際合作之契機。 | | | | | |
| **電子全文檔：** | C09804134_01.pdf | | | | | |
| **出國報告審核表：** | C09804134_A.doc | | | | | |
| **限閱與否：** | 否 | | | | | |
| **專責人員姓名：** | 劉昇平 | | | | | |
| **專責人員電話：** | 02-37073056 | | | | | |

# 出國報告審核表

## 出國報告審核表

<table>
<tr><td colspan="4">出國報告名稱：近海水文觀測與資料分析技術研習</td></tr>
<tr><td colspan="2">出國人姓名（2 人以上，以 1 人爲代表）</td><td>職稱</td><td>服務單位</td></tr>
<tr><td colspan="2">王仲豪</td><td>副工程司</td><td>經濟部水利署</td></tr>
<tr><td>出國類別</td><td colspan="3">☑考察 ☐進修 ☐研究 ☐實習<br>☐其他_____（例如國際會議、國際比賽、業務接洽等）</td></tr>
<tr><td colspan="2">出國期間：98 年 10 月 19 日至 98 年 1 月 2 日</td><td colspan="2">報告繳交日期：98 年 12 月 21 日</td></tr>
<tr><td>計畫主辦機關審核意見</td><td colspan="3">☑1.依限繳交出國報告<br>☑2.格式完整（本文必須具備「目的」、「過程」、「心得及建議事項」）<br>☑3.無抄襲相關出國報告<br>☑4.內容充實完備<br>☑5.建議具參考價值<br>☑6.送本機關參考或研辦<br>☑7.送上級機關參考<br>☐8.退回補正，原因：☐不符原核定出國計畫 ☐以外文撰寫或僅以所蒐集外文資料爲內容 ☐內容空洞簡略或未涵蓋規定要項 ☐抄襲相關出國報告之全部或部分內容 ☐電子檔案未依格式辦理 ☐未於資訊網登錄提要資料及傳送出國報告電子檔<br>☑9.本報告除上傳至出國報告資訊網外，將採行之公開發表：<br>☑辦理本機關出國報告座談會（說明會），與同仁進行知識分享。<br>☐於本機關業務會報提出報告<br>☐其他_____<br>☐10.其他處理意見及方式：</td></tr>
<tr><td>審核人</td><td>一級單位主管<br>水文技術組組長陳肇成</td><td colspan="2">機關首長或其授權人員</td></tr>
</table>

說明：

一、各機關可依需要自行增列審核項目內容，出國報告審核完畢本表請自行保存。

二、審核作業應儘速完成，以不影響出國人員上傳出國報告至「政府出版資料回應網公務出國報告專區」爲原則。

# 摘要

本次赴德國GKSS研究中心進行15天之「近海水文觀測與資料分析技術研習」，係獲98年度經濟部國際合作處台德技術合作人員訓練計畫核定。研習內容有雷達遙測原理、雷達遙測技術之進展、雷達遙測應用於海洋現象觀測、GKSS中心研發之雷達遙測資料分析數值模式-Disc介紹、現地觀測站作業觀摩與討論及現地觀測站之管理與維護方式之研習等。在爲期15天之研習時間，吸收GKSS研究中心應用雷達技術進行近海水文觀測作業之原理，以及雷達觀測資料之核心分析技術及模式，並藉由觀摩4處岸基雷達觀測站及其維護管理作業，獲得關於岸基雷達系統更爲詳細之運作流程。本次研習已初布獲得可茲水利署於未來發展非接觸式近海水文觀測技術之參考，以及我國與德國海岸工程研究機構，未來進一步進行國際合作之契機。

# 目錄

# 圖目錄

# 表目錄

# 謝誌

本(98)年度經濟部國際合作處台德技術合作人員訓練計畫赴德國進行為期15天之「近海水文觀測與資料分析技術研習」，承蒙該處　趙孟華小姐及　張玉燕小姐之行政協助，水利署同仁、長官協助分擔工作，駐德國代表處經濟組鍾秘書昇宏與駐慕尼黑辦室處商務組(法蘭克福)　鄭錦松先生等提供該國近況及需注意事項等資訊，並在國立成功大學水利工程學系　高教授家俊與　吳博士立中之推薦及協助連繫下，順利獲德國GKSS研究中心邀請函，遂得以順利成行。在德國研習過程中，獲GKSS中心海洋研究學院雷達水文技術研發部　Dr. Freidwart Ziemer率領之研究團隊的接待，並於參訪期間由其團隊成員，Stephan Sedlacek, Gottfried Schymura, Jörge Seemsn, Marius Cysewski, Stylianos Flampouris等，每日之陪同與詳盡解說，使得本次研習行程得以順利圓滿達成，另在回國時再獲駐慕尼黑辦室處商務組(法蘭克福)　沈組長長進及　鄭錦松先生之協助，順利搭機返國，在此謹致上最誠摯的謝意。

# 壹、前言

近海水文資料包含潮位、波浪、海流、漂砂等，爲本署海堤區域禦潮防災業務執行之重要基本資料，爰此，水利署署依據院核定之「台灣地區水文觀測現代化整體計畫」建置近海水文站網，目前所提供之觀測資料有潮位、波浪、氣溫、氣壓等，惟近海海流、漂砂、碎波帶等資料，因受限經費與國內現有技術能力，尚無法全數進行全天候觀測作業，僅能應用相關之資料分析，進行推估或模擬分析，其所得之結果僅部分能提供海堤區域禦潮防災業務之參考。爲找尋突破上述業務執行之瓶頸，於本(98)年度在獲經濟部支持之下，以核定天數15天(98年10月19日至11月2日)之時間，赴德國GKSS(Gesellschaft für Kernenergieverwertung in Schiffbau und Schifffahrt)研究中心，汲取其在近海水文觀測技術與資料分析(如雷達遙測、雷達觀測站之管理與維護、觀測資料品管與分析等)等領域之經驗與觀念，並冀能吸收其最新技術能力，提供本署在執行近海水文觀測及禦潮防災業務之參考。

# 貳、研習行程

## 2.1 行程資料

本次研習行程詳列如表 1，主要研習內容有雷達遙測原理、雷達遙測技術之進展、雷達遙測應用於海洋現象觀測、GKSS 中心研發之雷達遙測資料分析數值模式-Disc 介紹、現地觀測站作業觀摩與討論及現地觀測站之管理與維護方式之研習等，研習時間共計 15 天(98 年 10 月 19 日至 11 月 2 日)，地點爲位於 Schleswig-Holstein(什列斯威-豪斯敦州，亦有譯爲石勒蘇益格－荷爾斯泰因州，簡稱石－荷州)之 Geesthacht(吉斯哈赫特)之 GKSS 研究中心，與其雷達觀測站現址，比蘇姆 (Büsum)及夕爾特島(Sylt Island)，訪談對象爲該中心海岸研究學院雷達遙測技術研發部(Institute for Coastal Research / Department Radar Hydrography) Ziemer 博士。

表1　研習行程表

| 訓練進修日期及時間 | 訓練進修地點 | 實際訓練進修機構及訪談對象 | 訓練進修目的及討論主題 |
|---|---|---|---|
| 10 月 19 日 | 台北→法 蘭克福→漢堡→吉斯哈赫特 (Taipei → Frankfurt → Hamburg → Geesthacht) | 1.Institution:<br>GKSS 研究中心海岸研究學院 (Institute for Coastal Research, GKSS Research Center)<br>2.Person to be visited:<br>Dr. Friedwart Ziemer,<br>3.Contact person:<br>Dr. Friedwart Ziemer, GKSS-Research Center, Institute for Coastal Research / Radar Hydrography (KOR), Max-Planck-Straße 1, D-21502 Geesthacht, Schleswig-Holstein, Germany (吉斯哈赫特,什列斯威-豪斯敦)<br>Tel: 49(0) 4152-87-2827<br>Fax: 49(0) 4152-87-2818<br>E-mail:<br>friedwart.ziemer@gkss.de | 抵達吉斯哈赫特拜會 GKSS 研究中心 Dr. Friedwart Ziemer 帶領之海岸研究學院之雷達遙測技術研發部並瞭解 GKSS 概況<br><br>討論主題<br>雷達遙測原理之瞭解 |
| 10 月 20 日 | 吉斯哈赫特 (Geesthacht) | 同上 | 討論主題<br>1.簡介本署近海水文觀測現況<br>2.GKSS 應用雷達遙測進行海洋觀測之現況 |
| 10 月 21 日 | 吉斯哈赫特 | 同上 | 討論主題 |

| | | | |
|---|---|---|---|
| | (Geesthacht) | | 雷達遙測應用於各種海洋現象觀測之準確度探討 |
| 10 月 22 日 | 吉斯哈赫特<br>(Geesthacht) | 同上 | 討論主題<br>當前國外雷達遙測技術應用於海洋觀測及航運之進展 |
| 10 月 23 日 | 吉斯哈赫特<br>(Geesthacht) | 同上 | 討論主題<br>研習雷達遙測結果與數值模式-Disc 之整合 |
| 10 月 24-25 日 | 吉斯哈赫特<br>(Geesthacht) | | 1.週末<br>2.整理及準備下週研習資料 |
| 10 月 26 日 | 吉斯哈赫特→比蘇姆→吉斯哈赫特<br>(Geesthacht → Büsum → Geesthacht) | 1.Institution:<br>GKSS 研究中心海岸研究學院比蘇姆及夕爾特島雷達觀測站<br>(Radar Observation Stations in Büsum and Sylt Island of Institute for Coastal Research, GKSS Research Center)<br>2.Person to be visited:<br>Dr. Friedwart Ziemer,<br>3.Contact person:<br>Dr. Friedwart Ziemer, GKSS-Research Center, Institute for Coastal Research / Radar Hydrography (KOR), Max-Planck-Straße 1, D-21502 Geesthacht, Schleswig-Holstein, Germany<br>(吉斯哈赫特,什列斯威-豪斯敦)<br>Tel: 49(0) 4152-87-2827<br>Fax: 49(0) 4152-87-2818<br>E-mail:<br>friedwart.ziemer@gkss.de | 討論主題<br>雷達測流系統觀測站之管理與維護方式之研習(1/5) |
| 10 月 27 日 | 吉斯哈赫特→夕爾特島<br>(Geesthacht → Sylt Island) | | 討論主題<br>1.雷達測流系統現場作業方式之觀摩與討論(1/4)<br>2.雷達測流系統觀測站之管理與維護方式之研習(2/5) |
| 10 月 28 日 | 夕爾特島<br>(Sylt Island) | | 討論主題<br>1.雷達測流系統現場作業方式之觀摩與討論(2/3)<br>2.雷達測流系統觀測站之管理與維護方式之研習(3/5) |

| | | | |
|---|---|---|---|
| 10 月 29 日 | 夕爾特島<br>(Sylt Island) | | 討論主題<br>1.雷達測流系統現場作業方式之觀摩與討論(3/3)<br>2.雷達測流系統觀測站之管理與維護方式之研習(4/5) |
| 10 月 30 日 | 夕爾特島→漢堡→法蘭克福<br>(Sylt Island→ Hamburg→ Frankfurt) | | 討論主題<br>1.雷達測流系統觀測站之管理與維護方式之研習(5/5)<br>2.GKSS 於近海水文觀測創新技術引進我國之可行性討論<br>(晚間自漢堡搭機至法蘭克福轉機準備返台，並整理研習期間蒐集之資料) |
| 10 月 31 日 | 法蘭克福<br>(Frankfurt) | | 1. 週末移動日，爲配合班機時間，宿轉機地點法蘭克福<br>2. 整理研習期間蒐集之資料 |
| 11 月 1-2 日 | 法蘭克福→台北<br>(Frankfurt→ Taipei) | | 返程回台北 |

## 2.2 GKSS中心簡介

GKSS 研究中心(Gesellschaft für Kernenergieverwertung in Schiffbau und Schifffahrt Forschungszentrum) 是德國研究中心赫蒙霍茲協會(Helmholtz-Gemeinschaft Deutscher Forschungszentren)所屬 15 個研究中心之一，成立於西元 1956 年，目前 GKSS 研究中心有 2 處園區，分別位於位於 Schleswig-Holstein(什列斯威-豪斯敦州，亦有譯爲石-荷州)之 Geesthacht(吉斯哈赫特)，以及鄰近柏林的 Teltow(泰爾托)，現有研究人員約 800 人。

GKSS 研究中心主要從事海岸方面的研究以及先進工程材料的開發，同時也發展醫學工程與技技和物質結構方面的科學研究工作，並亦從事國際性研發工作，該中心所獲得之研究成果多能付諸於工業，故其與工業界和德國公家機構常有密切合作之關係。

目前 GKSS 研究中心之研究重點有，海洋、海岸與極地研究(Marine, Coastal and Polar Research)、先進工程材料(Advanced Engineering Materials)、大尺度中子、光子與離子研究設備(Large-Scale Facilities for Research Photons, Neutrons and Ions)與再生醫學(Regenerative Medicine)等 4 項，分別由其下設之海岸研究學院(Institut für Küstenforschung ; Institute for Coastal Research)、聚合物研究學院(Institut für Polymerforschung ; Institute of Polymer Research)、材料研究學院(Institut für Werkstoffforschung ;Institute of Materials Research)及 Geesthacht 中子設施所(Neutronen für die Wissenschaft GeNF; Geesthacht Neutron Facility, GeNF)執行之。

近年來，由於氣候改變及海面上升，使沿海地區成爲矚目地帶。GKSS 研究中心的海岸研究學院人員特別注重北德地區的氣候，以及德國接鄰之北海(Nordsee; North Sea)、波羅的海(Ostsee; Baltic Sea)區域。對北海、波羅的海區域而言，暴風的級數、海浪強度以及風暴潮都是形成暴風的重要因素，對歐洲北部的經濟和環境具有密切的因果關係，遂進行定期監測與評估德國北海與波羅的海之水質。因此 GKSS 研究中心的科學家針對此任務發展一項新的監測方法。除此之外，格陵蘭附近之極地海域生態系統的生物結構分析及其化學互動情況也是本中心科學家的研究議題，此項研究可以正確測知海岸地區的真實狀況。

以材料創新達到生產創新，是未來科技的基礎。爲了要永續性地充分利用資源、能源以及醫學技術，GKSS 研究中心材料研究學院進行先進工程材料之研發，例如交通與能源科技輕構造所需的金屬與聚合材料，以及成分解析過程、醫學科技或化學科技的催化作用所需要的以聚合物爲基礎的組件系統(components system)。

再生醫學是 GKSS 研究中心具有未來潛力的一項研究，由位於柏林近郊 Teltow 園區執行。GKSS 研究中心之聚合物研究學院在材料研究及組織工程方面的研究成果，可以提供較有效的治療方法，以幫助器官失靈或受損的病患。生物混合系統或生物兼容與生物功能性材料可以在人體內執行某些特定的功能，這就成爲科學家在此領域的基本研發工作，他們的目標是製造出一個運作正常的代用器官，如人工腎臟等。

有關大尺度中子、光子與離子研究設備方面，GKSS 研究中心之 Geesthacht 中子設施所擁有一座名爲 FRG-1 的研究反應爐，可以進行任何基礎研究及材料檢測等工作。該反應爐利用中子探測受測材料的內部結構。不管是玻璃、陶瓷、塑膠、金屬、蛋白質、氨基酸或磁性結果，均不會造成任何損壞或改變。

有關 GKSS 中心組織架構(含行政及研發部門等)，如圖 1 所示。

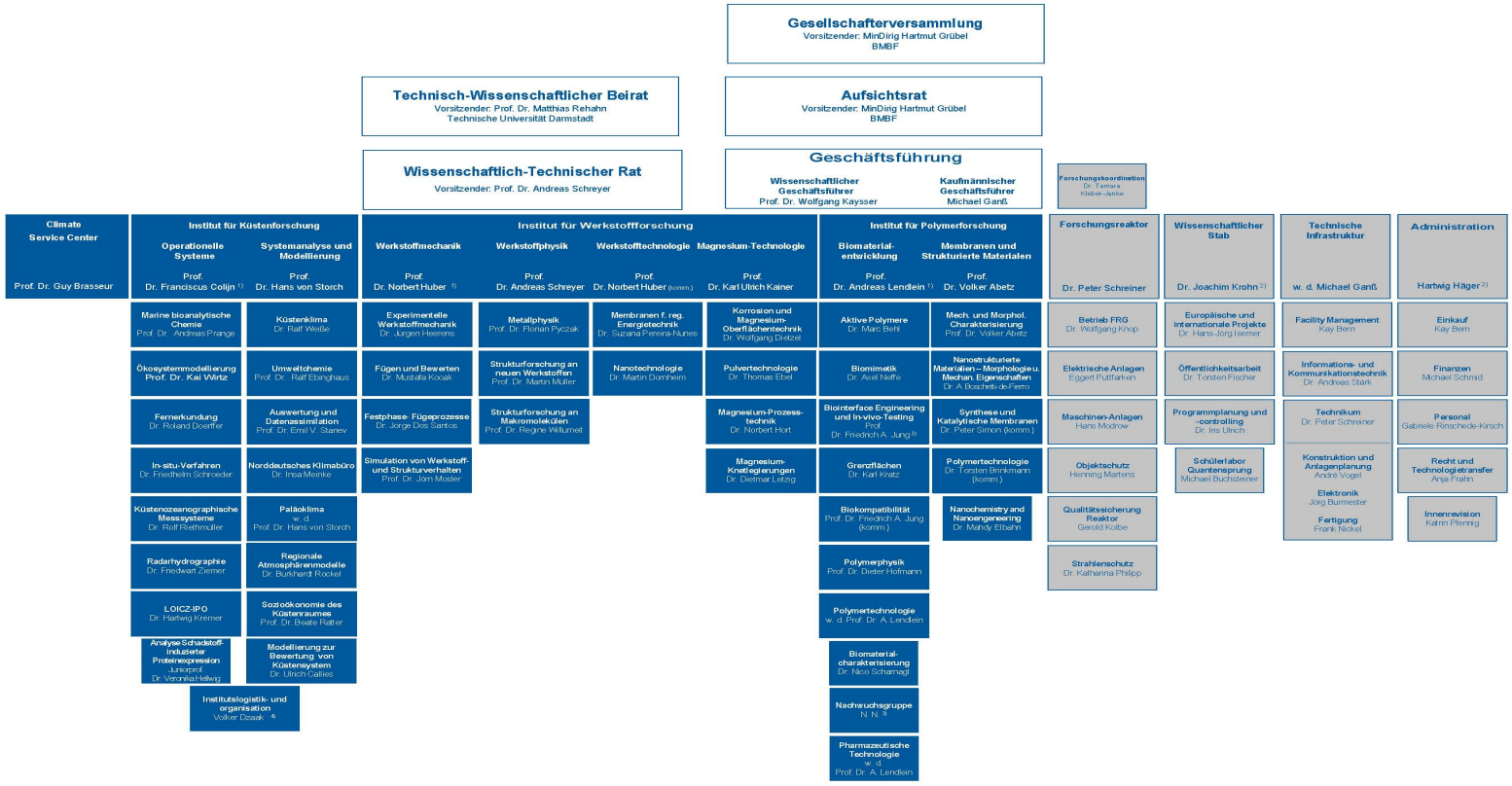


圖 1　GKSS 研究中心組之架構圖(德文，資料來源：GKSS)

本次研習地點爲位於 Geesthacht 之園區(GKSS Forschungszentrum Geesthacht)，如圖 2。

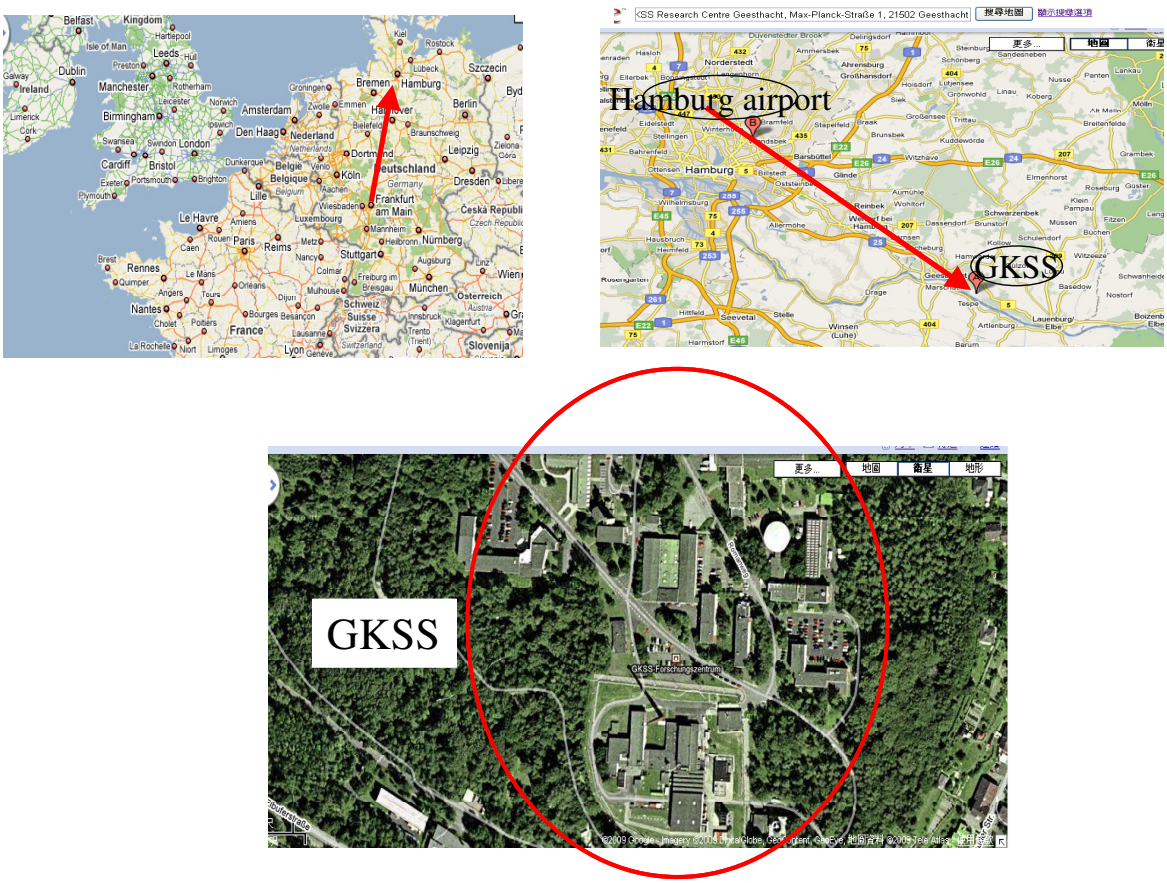


圖 2　GKSS 研究中心 Geesthacht 園區位置圖(底圖來源：Google 地圖)

## 2.3 GKSS中心海洋研究學院

GKSS中心海洋研究學院，圖3，目前由3個研究小組組成，分別爲系統分析與模擬組(System Analysis and Modeling)，操作系統發展組(Development of Operational Systems)，以及管理與系統組(Logistics and Organisation)。其中系統分析與模擬組擁有海岸氣候(Coastal Climate)、區域性大氣模擬(Regional Atmospheric Modelling)、海岸系統評估模擬(Modelling for the Assessment of Coastal Systems)、資料分析與資料同化(Data Analysis and Data Assimilation)、古氣候學(Paleoclimatology)、環境化學(Environmental Chemistry)、海岸人文區域(Human Dimension of Coastal Areas)等7個技術研發部門；操作系統發展組亦有7個分支技術研發部門，分別爲雷達水文(Radar Hydrography)、遙感探測(Remote Sensing)、海岸地行測量系統(Coastal Oceanographic Measurement System)、現地測量(In situ Measurements)、生態系模擬(Ecosystem Modelling)、海洋生物化學(Marine Bioanalytical Chemistry)以及污染對蛋白質反應分析(Analysis of pollutant-induced protein expression)。

圖 3　GKSS 中心海洋研究學院

本次研習係參訪操作系統發展組，由Dr. Friedwart Ziemer主持之雷達水文技術研發部(Radarhydrographie；Radar Hydrography)，有關Dr. Ziemer個人及其主持之雷達水文技術研發部目前研究內容，茲簡要介紹如下。

2.3.1 主持人Dr. Ziemer 簡介

Dr. Ziemer 全名爲 Friedwart Ziemer，圖4，德國漢堡大學地球科學(geosciences)博士，現爲GKSS研究中心海洋研究學院雷達水文技術研發部的主持人。Dr. Ziemer 從事海洋科學的研究已二十餘年，專長爲海洋遙測技術以及數值模式，其於1978開始進行波浪、海流之相關研究，初期僅由他1人進行資料觀測與分析，以及儀器維護管理等工作，後來漸漸有研究工作伙伴加入後，始有研究團隊成形，直至進入GKSS研究中心海洋研究學院主持雷達水文技術研發部後，其研究團隊便著重在應用雷達系統於近海水文觀測技術之研發，並成功研發出幾項不同的雷達觀測技術，從中獲得波浪、海流等重要海洋 (包含近海區域) 資訊。

Dr. Ziemer 現在及過去執行過多項德國以及歐盟之大型國際合作研究計畫，如COSYNA (Coastal Observation System for Northern and Arctic Sea), OROMA (Operational Radar and Optical Mapping in monitoring hydrodynamic, morphodynamic, and environmental parameters for coastal management), HYMNE (Hydrographic Monitoring of the Neva Bight )等。除研究工作外，Dr. Ziemer亦定期在德國漢堡大學與基爾大學講學，教授海洋觀測學。從1990年至今，他共發表了近40篇的學術研究文章，其中包含了9篇的專書與期刊論文，29篇的國際研討會論文。此外，Dr. Ziemer擁有3項海洋觀測技術之專利權。


圖 4　與 Dr. Ziemer 合影(拍攝於雷達水文技術研發部，2009)

2.3.2 雷達水文技術研發部目前研究內容

GKSS研究中心海洋研究學院之雷達水文技術研發部，目前由Dr. Ziemer所率領，研究人力現爲7人，其研究重點爲應用雷達系統進行北海地區之海洋水文現象觀測與分析，如波浪、海流等，該部門目前擁有5座雷達觀測站，分別位於比蘇姆(Büsum)、夕爾特島(Sylt Island)及北海海域，其中位於比蘇姆(Büsum)及夕爾特島(Sylt Island)之4處雷達觀測站屬於岸基雷達系統，其使用之觀測波段有HF及X頻段(X-band)2種；至於雷達系統所觀測到之現地資料，由其所研發之DiSC(Dispersive Surface Classifier)模式進行處理與分析。現階段雷達水文技術研發部之研究重點有4項，茲臚列如下：

(1)應用雷達技術進行波浪與海流觀測(routine current and wave observation)。

(2)應用雷達技術進行水深觀測(observation of the bathymetry)。

(3)近岸地區波浪能量衰減研究(research on littoral wave energy decay)。

(4)波浪與海流及海流與底床砂丘交互作用之研究 (research on wave - current and current - bottom (sand) interaction)。

# 參、研習內容

本次研習內容可歸納爲雷達遙測原理及其於海洋觀測之應用、GKSS 研究中心研發之雷達遙測資料分析數值模式-DiSC、雷達觀測站及其管理維護作業之觀摩，以及與 GKSS 進行國際合作可行性討論等項目。

## 3.1 雷達遙測原理及其於海洋觀測之應用

### 3.1.1 雷達遙測原理

雷達（RADAR）一詞爲 Radio Detection And Ragning 縮寫，其意義乃利用目標物對電磁波(頻率爲高於 1MHz)的散射特性測定目標物在空間中的位置，並藉由都卜勒位移(Doppler shift)獲取方位方向（Azimuth Direction）高解析度，並於同時對於目標物的距離方向（Range Direction）以能分辨目標物在不同距離上的解析能力，使得回波信號能在方位方向與距離方向產生耦合(coupled)。

雷達是一種主動微波感測器，具備不受天候與日照條件影響之優勢，提供電磁波頻譜中微波波段的訊號特性，可從不同載具（空載或衛載或岸基）、極化（單偏、多偏極或全偏極）、波段（X 波段至 L 波段）進行地表觀測，因此其優越性被國內外廣泛應用於軍事和民用，如海洋物理、海洋污染、地殼變形、山坡地滑動、目標物移動等議題上的研究。本次研習內容涉及爲雷達應用於海洋科學之研究，有關雷達應用近海水文觀測之機制與原理，茲說明如下。

雷達的回波機制可分爲兩部份探討，當雷達入射海面角度幾近垂直時，此時雷達回波強度主要受水面鏡面反射產生；若是當雷達波入射角度甚低(EM 波與海面夾角小於 10 度)，稱爲低掠角(low grazing angle)時，由於 X-band 波長與海面上的毛細波長相當，當雷達波由天線發射後抵達海面，當與海面毛細波滿足布拉格共振機制的條件時，雷達波產生反射。岸基 X-band 影像雷達應用上述海面背向散射機制進行海面環境之遙測，一般岸基雷達天線高度甚低，入射海面角度也小，皆爲低掠角狀況。

海面上因爲波浪之存在使海水表面起伏，雷達入射至海面時與海水面的入射交角皆不同，由布拉格共振條件可知，交角之改變影響是否產生回波，據此影響回波量的強度。因此海面海雜波的因波浪週期性的水位變動產生週期性的強度變動，在雷達屏幕上所見爲高灰度值的亮調紋與低灰度值之暗條紋交相出現的影像，形成了波紋，由上述低掠角雷達回波機制可知，此波紋長度與方向確與波浪一致，波紋的影像經由二維傅立葉轉換可推算波浪場之波數向量譜。

在波高估算方面，雖波紋明亮的變化程度與波高無直接關係，但由於低掠角影響，波浪波峰會遮蔽雷達射線，使波峰後方受遮蔽的區域全然沒有回波強度，形成影像灰度值的陡變，波高或波浪振幅則可利用傳遞函數藉由黑暗區域的特性中推算，傳遞函數則由實驗之經驗值迴歸推算。有了波浪振幅與波數向量譜，則相對應於該觀測瞬間的波浪方向譜可以求得。另外基於布拉格共振與毛細波的強度有關，亦與海面粗糙度有關。

雷達約 1~2 秒迴旋一圈，每一圈可獲得 360 度的全景影像，在連續觀測下，可以紀錄這些影像在時間上的變化，影像中某一點在時間上的週期性變動可經由頻譜分析得到波浪的頻率，在海面流場爲 0 的條件下，波數向量與頻率應滿足波浪的分散關係式(Dispersion relationship)，波數(wave number)向量與頻率間的關係若不滿足分散關係式，則其差異量可用於逆演算(inverse calculation)推求出當時的海面流場。

### 3.1.2 雷達遙測於海洋觀測之應用

本次研習內容其中一項爲參訪 Dr. Ziemer 雷達水文技術研發部，研發之岸基雷達系統(Radar System Based on Coastal)，其此採用之波段爲 X 頻段(X-band)，頻率介於 9.41 GHz~ 10.50 GHz 之間，以及 HF 頻段，採用頻率有 5MHZ 及 50MHz 兩種。前述雷達系統之偵測原理是由雷達天線向水面發射雷達波，而水面的粗糙構造會使得雷達波產生布拉格散射（Bragg scatter），圖 5。當入射波的波長是浪狀介面波長的兩倍，就可以產生第一階的布拉格反射，$2\lambda_e = \lambda_s$，其中 $\lambda_s$ 是水面波長，$\lambda_e$ 是發射的雷達波長。若此浪狀介面移動的話，自然產生都卜勒效應(Doppler Effect)，反射波的頻率便會隨著浪狀介面的遠離或靠近而改變，由此可推算出相對的移動速度。


圖 5　布拉格散射（Bragg scatter）原理 (Dr. Ziemer 提供)

Dr. Ziemer 主持之雷達水文技術研發部應用此觀念，進行近岸波浪、表面海流等近海水文資料觀測，近年來已於德國鄰接北海之岸際設置 4 座岸基雷達觀測站，如圖 6 中紅點標註所示，進行近岸波浪、海流、水深地形、漂砂、雲霧擴散等觀測研究，圖 7 至圖 9。


圖 6　Dr. Ziemer 所屬岸基雷達觀測站分布圖(攝於雷達水文技術研發部)

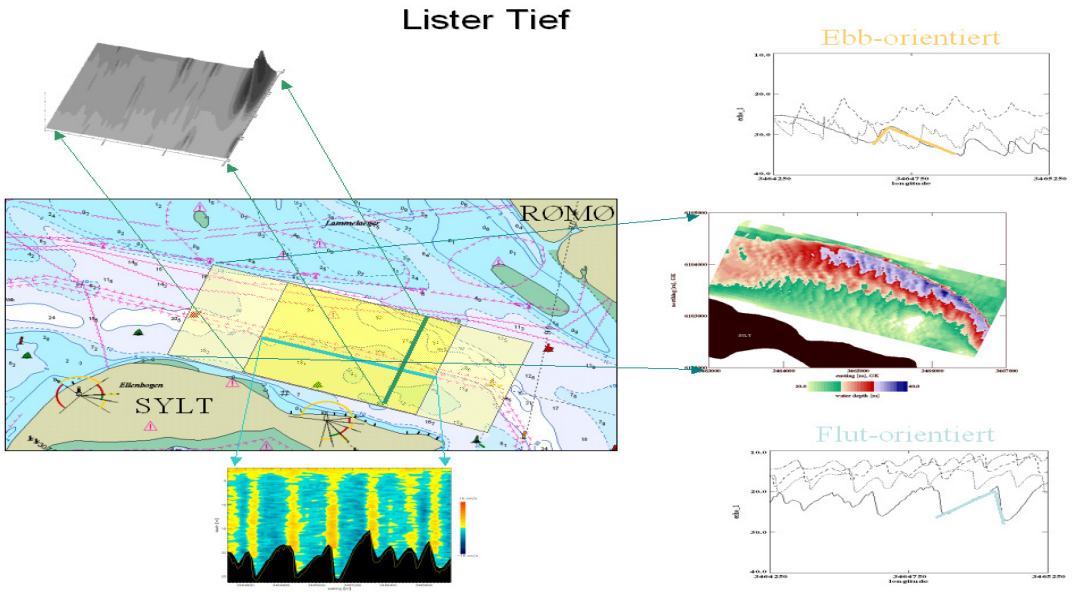


圖 7　岸基雷達應用於波浪、海流、水深地形之研究(Dr. Ziemer 提供)

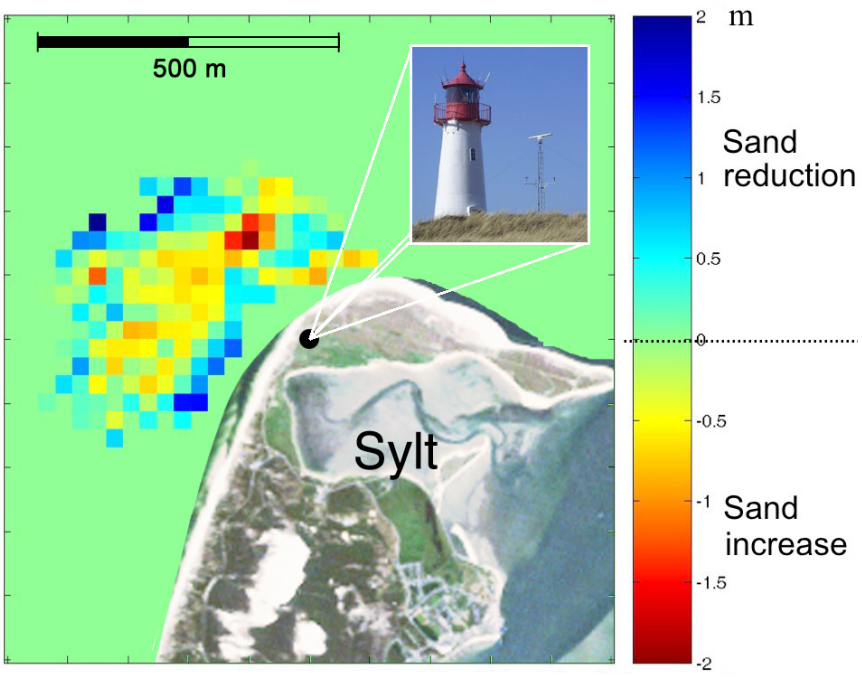


圖 8　岸基雷達應用於漂砂之研究(Dr. Ziemer 提供)

圖 9　岸基雷達應用於雲霧擴散之研究(Dr. Ziemer 提供)

## 3.2 雷達遙測資料分析數值模式-DiSC

雷達系統觀測所得之資料係爲影像資訊，Dr. Ziemer 主持之雷達水文技術研發部爲由雷達影像資訊獲得近岸海流、波浪、水深地形等資料，依據淺水域水深與流速線性分散性關係式，研發 DiSC(Dispersive Surface Classificator)模式進行前述研究工作之進行。

DiSC 模式核心分析技術爲應用 3 維快速傅立葉轉換(3-D Fast Fourier Transformation)進行雷達訊號轉換，再應用濾波原理萃取所需資訊後，以 2 維反快速傅立葉轉換(2-D Inverse Fast Fourier Transformation)產出觀測資料空間分布圖，並據以進行後續分析研究，圖 10，該模式經過不斷改良，目前(2009 年)已可解析雷達觀測資料之空間解析力至 7.5 米(2008 年時爲 40 米)，並可推算岸基雷達觀測資料離岸 1 至 2 公里範圍內之波浪、流速等近海水文參數，目前 DiSC 模式已完成圖形使用介面(GUI)之操作視窗，使得應用雷達觀測進行海水文資料觀測之處理程序更具便利性與親和性。有關 DiSC 之處理流及視窗介面如圖 11 至圖 12 所示。

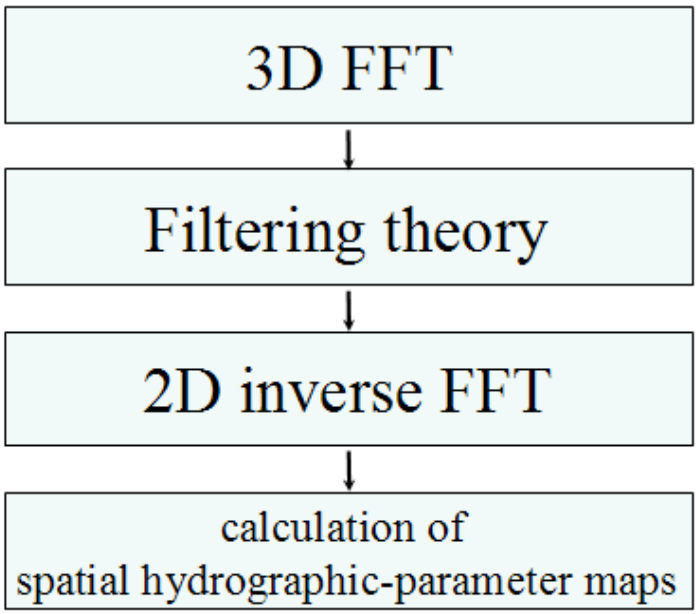


圖 10　DiSC 模式分析原理

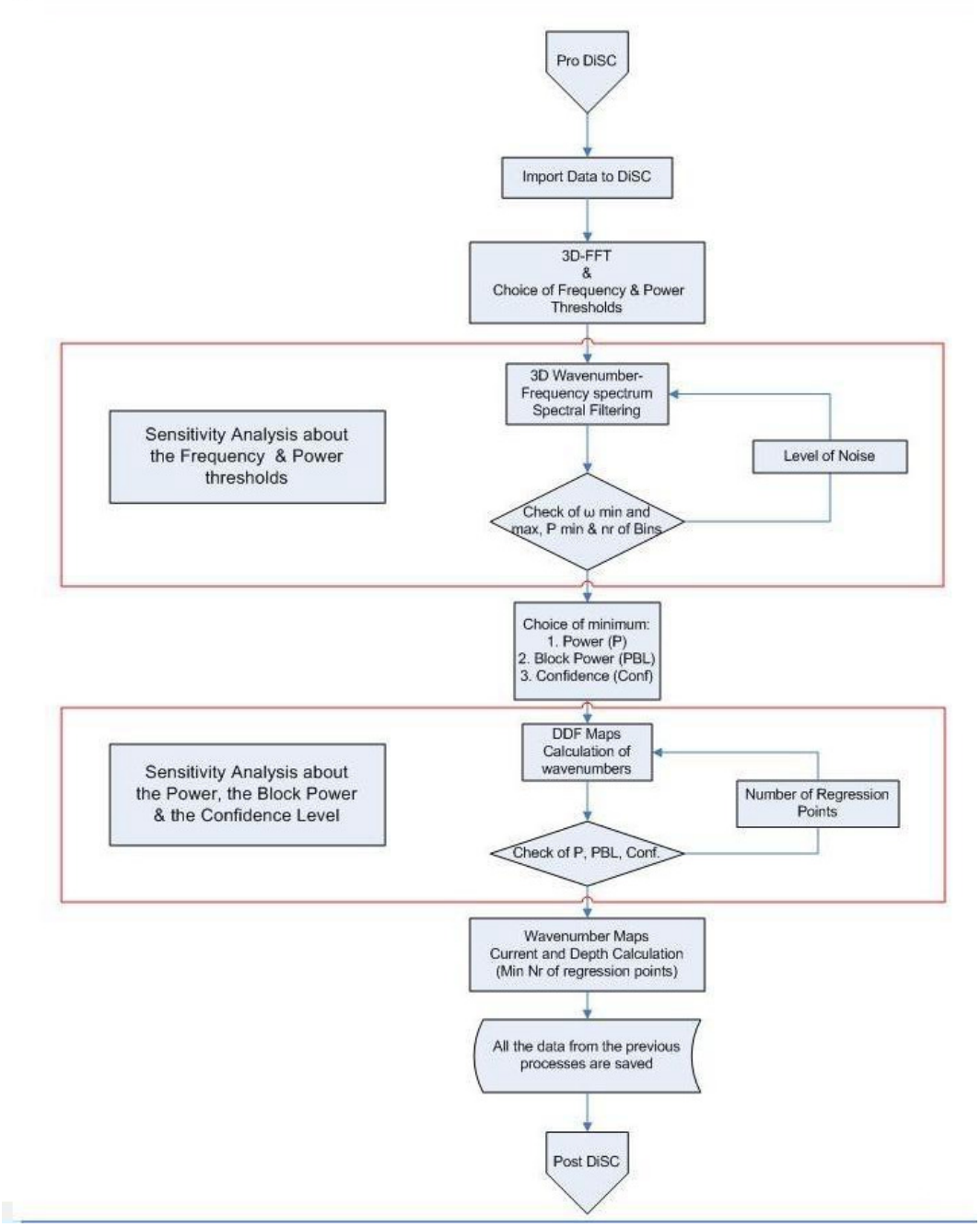


圖 11　DiSC 模式執行流程

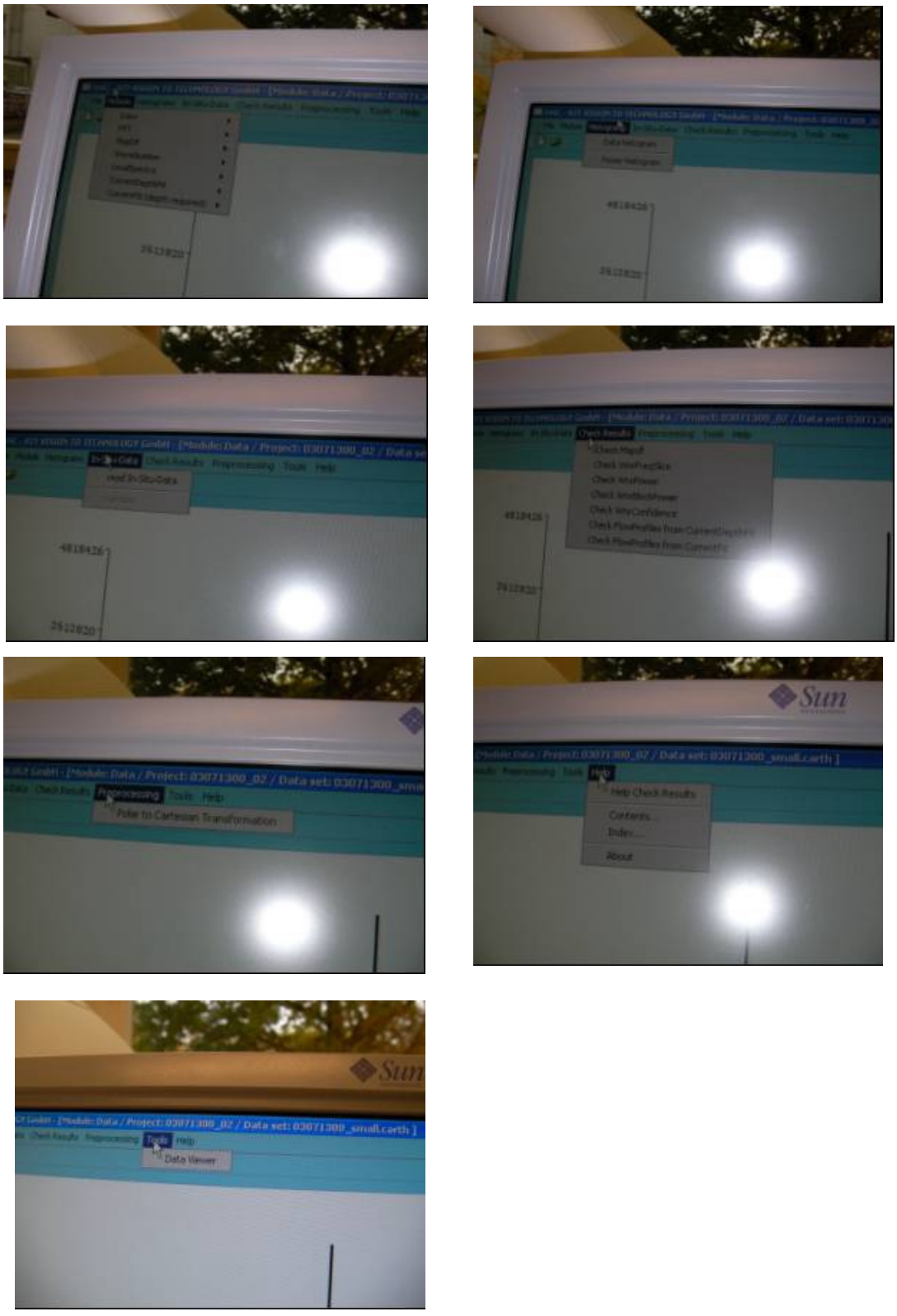

圖 12　DiSC 模式功能展示視窗

目前 Dr. Ziemer 研究團隊已將 DiSC 模式應用於水深觀測、近岸地區波浪能量衰減、波浪與海流及海流與底床砂丘交互作用等相關研究，如圖 13 及附錄。

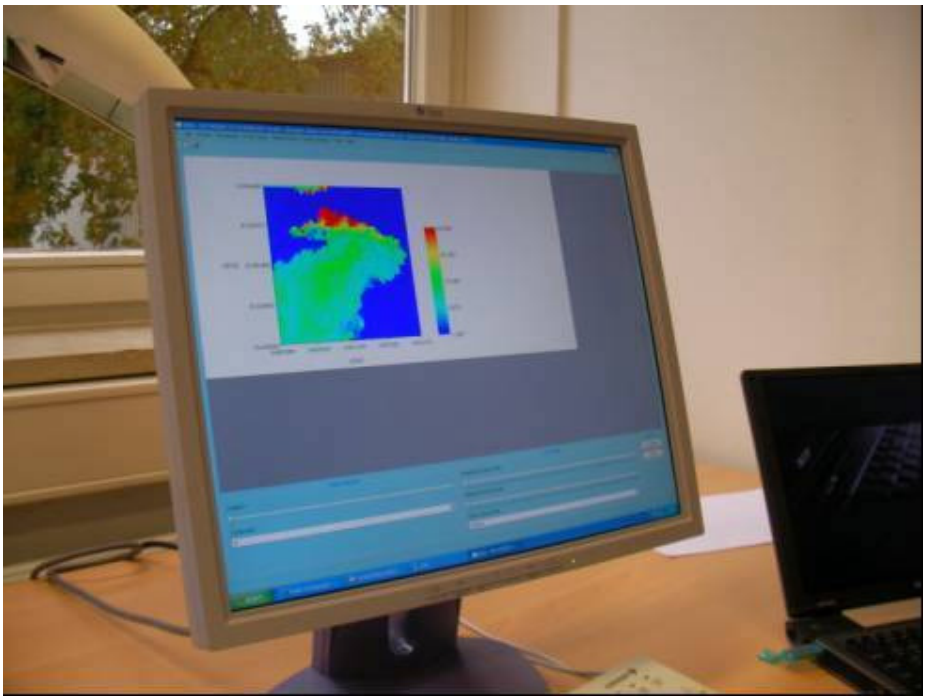

圖 13　應用 DiSC 推估近海區域水深資料

## 3.3 岸基雷達觀測站及其管理維護作業之觀摩

### 3.3.1 岸基雷達觀測站

本次研習除於 GKSS 研究中心進行室內研討外，亦於 10 月 26 日至 10 月 30 日，由 Dr. Ziemer 安排至德國北部鄰近北海地區之比蘇姆(Büsum)及夕爾特島(Sylt Island)，參觀 GKSS 研究中心設置之 4 處岸基雷達觀測站及觀摩其管理維護作業，此 4 處岸基雷達觀測站應用有 HF 頻段進行觀測有 2 處，分別位於比蘇姆(Büsum)及夕爾特島(Sylt Island)南端之 Rantum，另 2 處係使用 X 頻段(X-band)進行觀測，皆位於夕爾特島(Sylt Island)北部之利斯特(List)，其相關位置如圖 14。

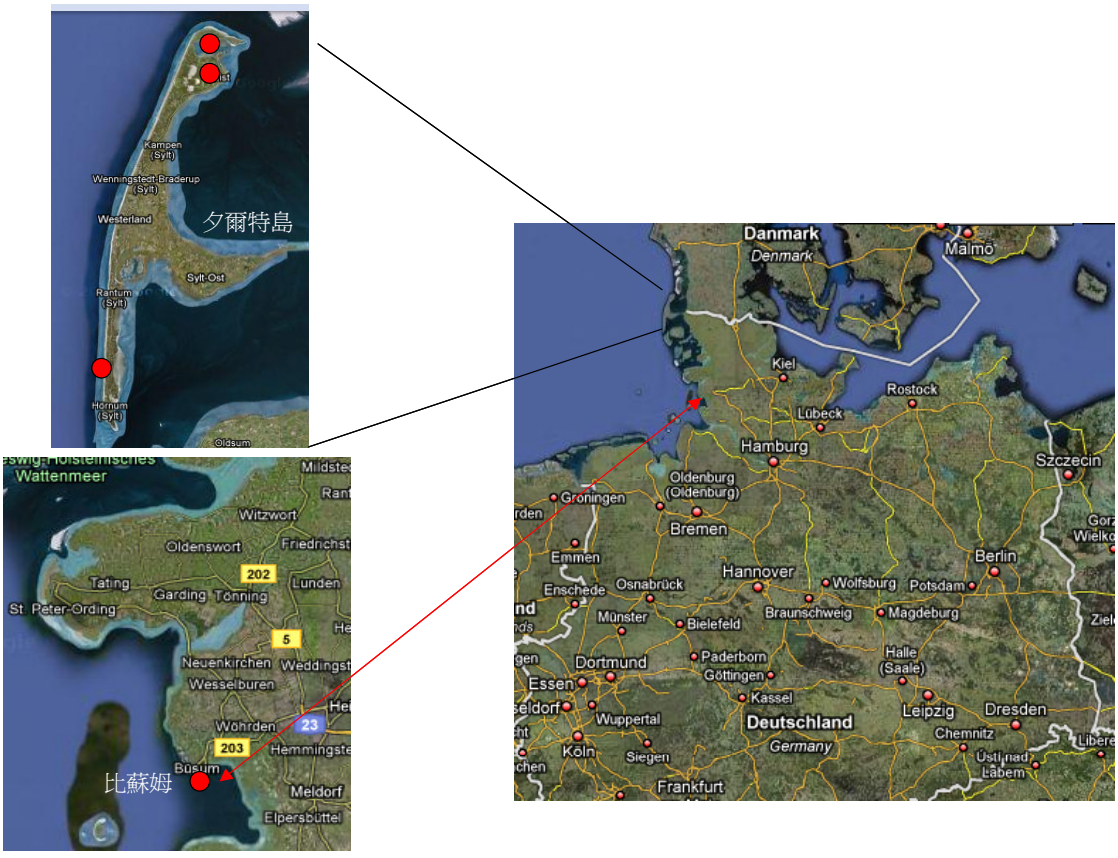


圖 14　本次研習參觀岸基雷達觀測站位置(紅點爲雷達觀測站，底圖來源：Google 地圖)

(1)比蘇姆(Büsum)岸基雷達觀測站

比蘇姆(Büsum)位於石－荷(Schleswig-Holstein)州北海海岸線上，屬於砂岸地形，爲 GKSS 研究中心執行 COSYNA(Coastal Observing System for Northern and Arctic Seas)計畫之重點區域之一。COYSNA 計畫主要執行內容爲執行德國與北極海岸觀測，並進一步進行相關觀測系統之整合，詳附錄，其中應用雷達觀測近海水文之工作係由 Dr.Ziemer 主持之雷達水文技術研發部負責。此處使用之雷達觀測系統爲 WERA(WavE RAdar)系統，屬於岸基雷達之類型，該系統使用 HF 頻段，觀測方法採用都卜勒原理，故本處之雷達站亦屬於都卜勒觀測雷達，此雷達觀測系統操作頻率爲 5MHZ 及 50MHz，雷達波型式爲有垂直極化(vertical polarised，VV)與水平極化(horizontal polarised，HH)，時間解析度爲 10 分鐘，最遠範圍爲 200 公里。本處岸基雷達觀測站之雷達波型式，係採用水平極化。

爲節省現地建站經費又可兼顧岸基雷達系統之安全性、機動性以及觀測與維護管理工作之便利性，Dr.Ziemer 採用貨櫃屋形式，建立本處雷達觀測站工作站房，雷達本體建置於貨櫃屋頂部，天線系統(含發射及接收系統)共 10 支，設置於貨櫃屋旁之岸上，分析系統置於屋內，平時採用遠端遙控方式進行觀測作業，如需人員至現場進行觀測與資料分析工作時，可藉由貨櫃屋金屬外殼之屏蔽效應，保護現地觀測與資料分析人員之安全。

本處岸基雷達觀測站採用之貨櫃屋大小爲 6 公尺長、2.5 公尺寬、2.5 公尺寬，觀測工作所需之電力源自於鄰近之燈塔，採用開放式之電攬線連接燈塔及貨櫃屋，故需定期進行電攬線維護工作，俾確保觀測系統所需之電力來源不發生中斷情形。有關比蘇姆(Büsum) 岸基雷達觀測站之外觀、內部，天線與線路等設置型式與架構等列如圖 15 至圖 20 所示。


圖 15　比蘇姆岸基雷達觀測站工作站房外觀

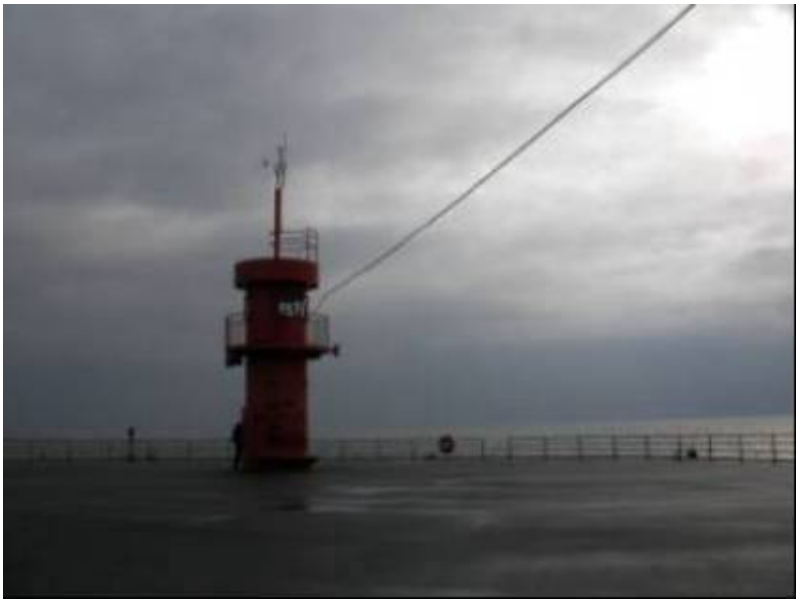

圖 16　比蘇姆燈塔(圖中電攬線爲岸基雷達觀測站電力來源)

圖 17　比蘇姆岸基雷達觀測站天線系統(含接收與發射系統)

圖 18　貨櫃屋工作站房內部及分析系統

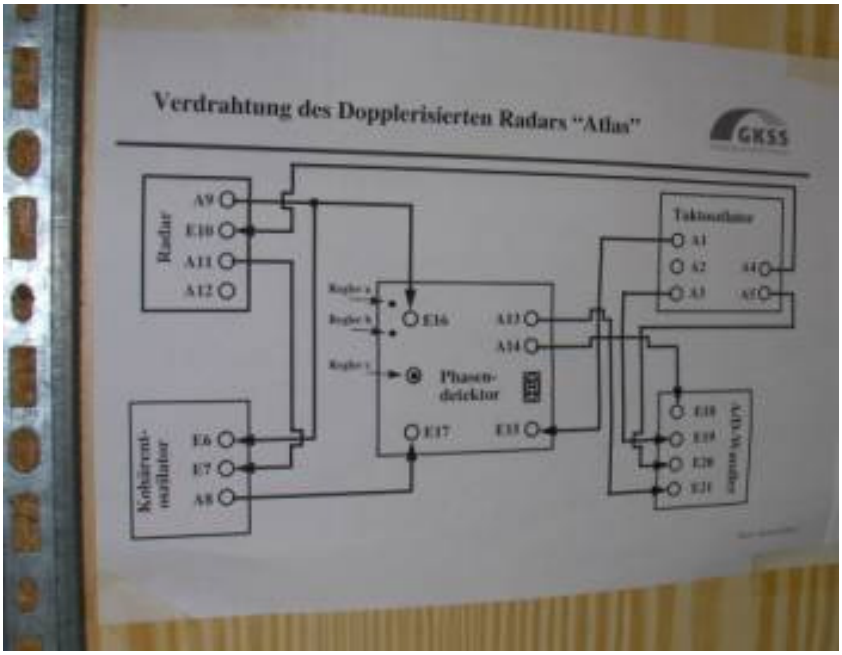


圖 19　比蘇姆岸基雷達觀測站線路圖

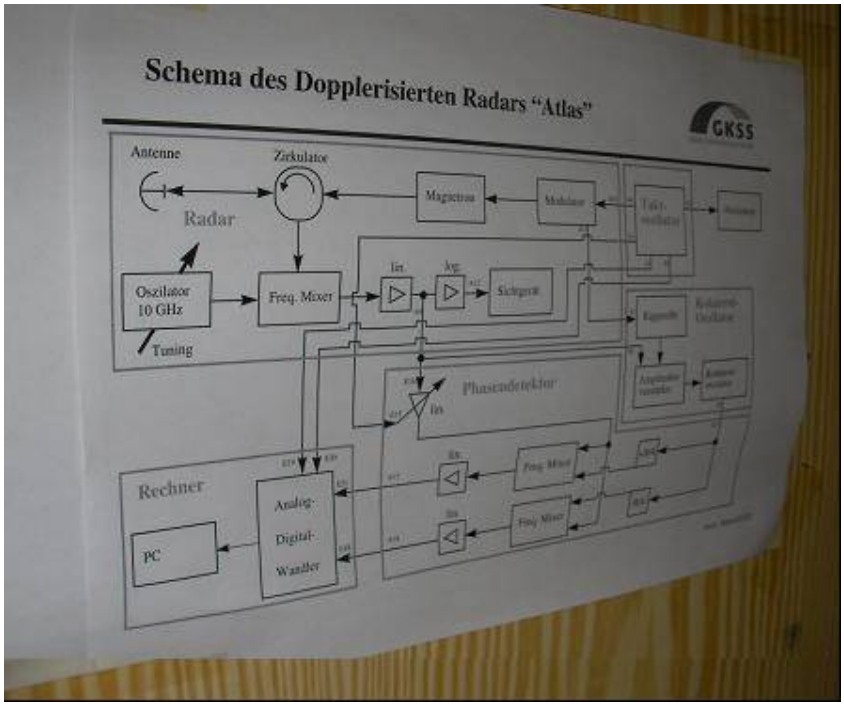


圖 20　比蘇姆岸基雷達架構圖

(2)夕爾特島(Sylt Island)岸基雷達觀測站

夕爾特島(Sylt Island)位於德國北方北海範圍內，鄰近丹麥，整座島多爲沙丘地形，是德國著名的渡假旅遊勝地之一，其著名的海灘每年吸引眾多遊客前往享受海上風情。

夕爾特島的海岸因受北海侵蝕威脅，過去德國政府曾採用工程手段，如築堤，設置消波塊等方式，藉以保全該島之海岸，但成效不彰，甚至加速夕爾特島沙質海岸的流失，德國政府目前以船運方式自外地運砂補充本地之灘，以持續維持本地的自然海岸環境及觀光效益。爲瞭解本區之海象變化，GKSS 研究中心將本區之近海觀測工作內容納入 COYSNA 計畫中，其中應用岸基雷達系統進行近海水文觀測之作業，交由 Dr.Ziemer 主持之雷達水文技術研發部負責。

本次研習於夕爾特島參觀 3 處岸基雷達觀測站，分別位於該島北端之利斯特(List)以及南端之 Rantum，其觀測原理皆爲應用都卜勒效應(Doppler Effect)，其中位於南端之 Rantum 岸基雷達觀測站，與比蘇姆使用同一系統，WERA(WavE RAdar)，雷達波型式同屬水平極化(horizontal polarised，HH)，亦採用貨櫃屋方式設置觀測站工作站房，但電力系統由市電供應電源，雷達天線共 16 支，其中雷達波發射(transmitter)天線有 4 支，接收(receiver)天線有 12 支，皆面向北海，主要任務爲觀測波浪及海流資料。

位於利斯特地區有 2 處岸基雷達觀測站，皆爲使用 X 頻段(X-band)進行觀測，波長爲 3 公分，屬於垂直極化(vertical polarised，VV)系統，其工作站房外觀型式採用拖車(trek)，雷達天線置於拖車旁之觀測高塔上，雷達之發射與接收天線架構於同一天線上，故天線體積較比蘇姆及 Rantum2 地之雷達系統輕巧，該觀測塔同時設置視訊影像、氣溫、風等觀測儀器，獲取進行觀作業時實際之海況(波浪及海流)及天氣資料，俾供雷達觀測結果比對之用，另該 2 處觀測站所得之雷達觀測資料，亦可藉由 DiSC 模式推估觀測區域進岸之水深地形分布情形。另觀測所需之電力，由太陽能板(共 18 塊)及置於拖車內部之發電機供應，其中發電機爲汽油驅動，需於定期維護工作進行時，適時添加油料。

Dr. Ziemer 於夕爾特島所設置之岸基雷達觀測站，皆可以遠端遙控進行觀作業，但 Dr. Ziemer 認爲如時間及天氣等條件許可下，觀測人員應進駐進行觀測工作，俾掌握雷達觀測資料之合理性。

有關夕爾特島利斯特(List)以及南端之 Rantum 岸基雷達觀測站之外觀、內部，天線與線路等設置型式與架構等列如圖 21 至圖 38 所示。

圖 21　List 南端岸基雷達站

圖 22　List 南端岸基雷達拖車工作站房(1)

圖 23　List 南端岸基雷達拖車工作站房(2)

圖 24　List 南端岸基雷達觀測塔

圖 25　List 南端岸基雷達拖車工作站房太陽能板

圖 26　List 南端岸基雷達拖車工作站房內部

圖 27　List 北端岸基雷達拖車工作站房

圖 28　List 北端岸基雷達站資料傳輸系統

圖 29　List 北端岸基雷達站風速風向觀測系統

圖 30　List 北端岸基雷達站觀測塔

圖 31　List 北端岸基雷達站站房內觀(1)

圖 32　List 北端岸基雷達站站房內觀(2)

圖 33　Rantum 岸基雷達觀測站

圖 34　Rantum 岸基雷達發射天線

圖 35　Rantum 岸基雷達接收天線

圖 36　Rantum 岸基雷達本體

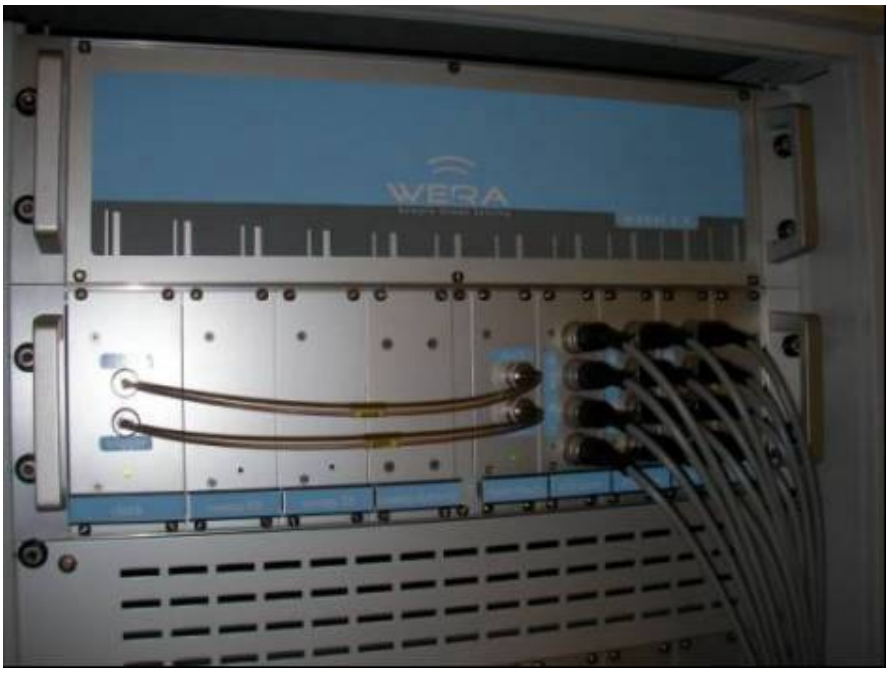


圖 37　Rantum 岸基雷達系統(WERA)

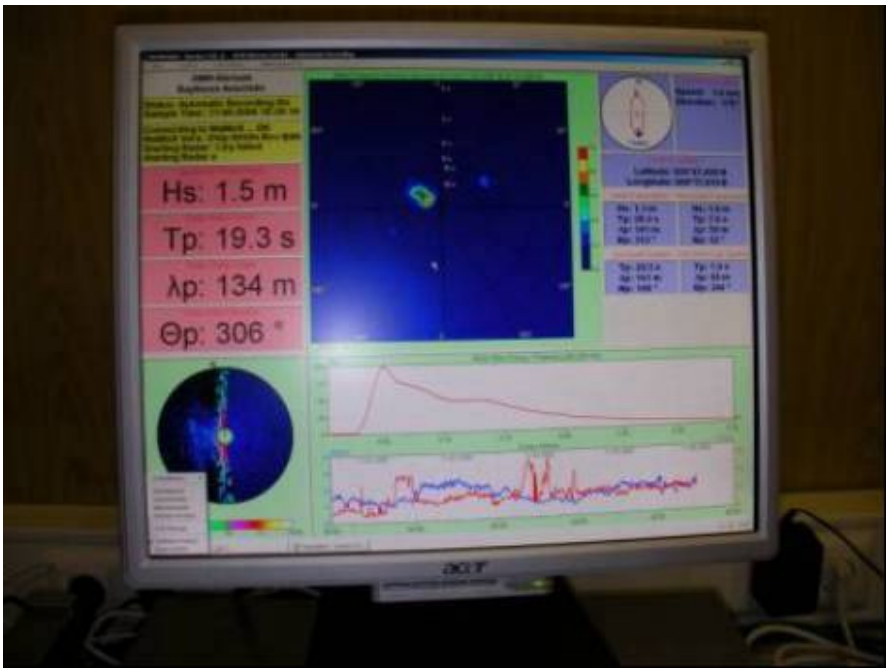


圖 38　Rantum 岸基雷達資料分析系統

### 3.3.2 岸基雷達觀測站管理維護作業觀摩

爲獲得可信及穩定之近海區域雷達觀測資料，Dr. Ziemer 研究團隊必須定期進行 GKSS 研究中心所屬之岸基雷達觀測站維護作業，以維持雷達觀測設備的正常運作功能。

本次研習期間適逢 Dr.Ziemer 主持之雷達水文技術研發部，進行雷達觀測站例行性維護作業行程，遂在 Dr. Ziemer 安排下，於參觀 GKSS 研究中心位於比蘇姆(Büsum)及夕爾特島(Sylt Island)之岸基雷達觀測站，亦同時觀摩雷達觀測站管理維護作業。

(1)比蘇姆(Büsum) 岸基雷達觀測站管理維護作業

本次適逢 Dr. Ziemer 研究團隊將對比蘇姆岸基雷達觀測站，進行電攬線檢查，便隨同 Dr. Ziemer 研究團隊之 Schymura 先生前往該站，進行維護作業，並於需要時給與適時協助。比蘇姆岸基雷達觀測站之電力來源，係源自於鄰近之燈塔，該燈塔電源屬市電，故比蘇姆(Büsum)雷達觀測站以電攬線之方式，串接該燈塔之市電，以提供該站進行觀測作業。兩者間之電攬線係以束帶固定，加上經年累月於戶外風吹雨淋，需進行定期檢查，並更換固定束帶，以確保電力供給不中斷，並維護至比蘇姆進行光觀之遊客安全。本次觀摩及協助作業內容如圖 39 至圖 45 所示。

圖 39　著工作服之 Schymura 先生

圖 40　安全繩索固定(比蘇姆岸基雷達觀測站)

圖 41　電攬線檢查(比蘇姆岸基雷達觀測站)

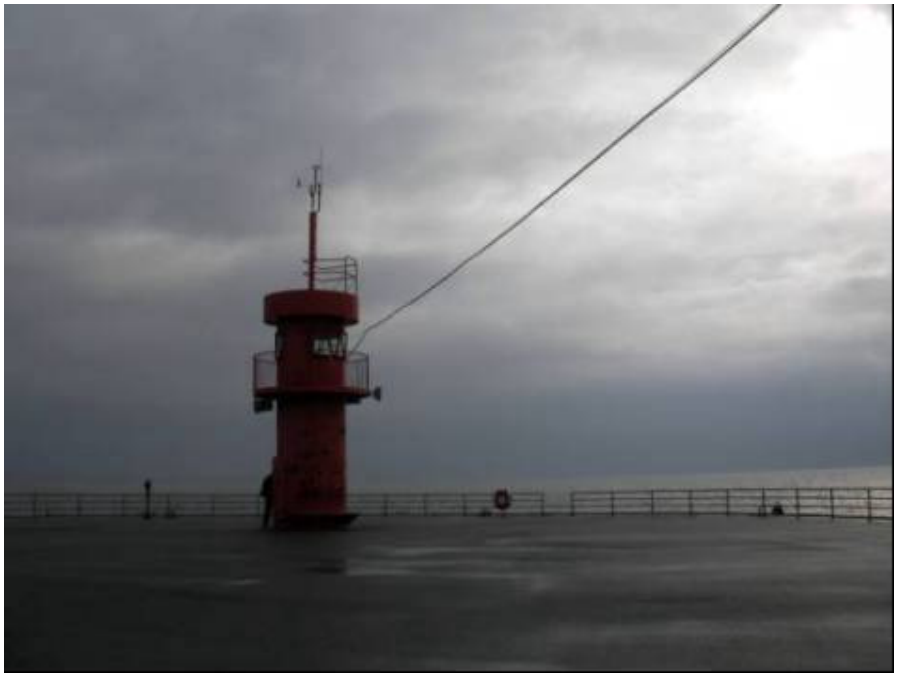

圖 42　燈塔(比蘇姆岸基雷達觀測站電力來源)

圖 43　觀測站端電攬線鬆綁

圖 44　電攬線束帶更新

圖 45　燈塔端電攬線束帶更新

(2) 夕爾特島(Sylt Island) 岸基雷達觀測站管理維護作業

GKSS 研究中心目前於夕爾特島設置 3 座岸基雷達觀測站，進行該島近海水文之觀測研究，俾掌握北海海況對於夕爾特島之影響，避免該島國土持續流失，同時亦爲執行 COSYNA 計畫之重點觀測站。本次觀摩之管理維護內容爲，檢修位於利斯特(List)南側之雷達天線硬體系統、定期保養位於利斯特(List)北側之雷達觀測站、以及檢測 Rantum 雷達觀測站。

位於利斯特(List)南側之雷達天線硬體系統，係位於拖車旁之高塔上，該塔高約 10 米，該硬體系統因不明原因無法運作，造成觀測工作中斷，故 Dr. Ziemer 率其同仁(Schymura 及 Sedlacek 先生)進行檢修，並必要時將予更換零組件。爲安全考量，Dr.Ziemer 團隊於進行雷達觀測站檢修工作時，需爲 2 人以上同行，檢修工作進行前，工作人員除需穿著工作服，圖 46，以保持身體溫暖及方便攜帶必要工具外，亦需確時作好攀至塔頂之相關安全措施，如安全繩索之扣環是否與觀測塔確實連接？是否與工作確實扣好？本站經 3 天之檢修，天線旋轉基坐(gear)僅更換部分固定螺絲，但雷達天線因與基座之連結系統發生故障，造成無法運轉，故經更換雷達天線後，已可順利運作，使該站之觀測任務得以持續。有關利斯特(List)南側之雷達天線系統，以及相關檢修工作內容，示如圖 47 至圖 53。

位於利斯特(List)北側之岸基雷達觀測站係於 2008 年 8 月設置，該站整體軟硬體系統較利斯特(List)南側之岸基雷達觀測站爲新。本次檢修內容爲定期保養該站之雷達觀測塔零組件是否有老舊或鬆脫，以及其它軟硬體設備是否可正常運作等情形，經檢查該站零組件無異常情形，雷達系統軟硬體運作功能正常。

位於夕爾特島(Sylt Island)南端 Rantum 岸基雷達觀測站，因觀測資料無法正常回傳，本次檢測內容即爲確認造成該站資料無法回傳之原因。經 Dr. Ziemer 確認後，該站雷達觀測軟硬體運作正常，觀測資料無法正常回傳之原因，係資料遠端傳輸系統出問題，因本次未攜帶足夠之傳輸系統零組件，Dr. Ziemer 決定另行安排修復工作。

有關夕爾特島(Sylt Island)3 處岸基雷達觀測站管理維護作業情形，如圖 46 至圖 55。

圖 46　維護作業服(Sedlacek 先生)

圖 47　List 南側岸基雷達觀測站維護作業(1)

圖 48　List 南側岸基雷達觀測站維護作業(2)( Sedlacek 先生)

圖 49　List 南側岸基雷達本體檢修(Schymura 先生)

圖 50　List 南側岸基雷達本體拆解(1)

圖 51　List 南側岸基雷達本體拆解(2)


圖 52　List 南側岸基雷達之基座

圖 53　岸基雷達之基座檢修(List 南側岸基雷達觀測站)

圖 54　List 南側岸基雷達觀測站維護作業(Schymura 先生)

圖 55　Rantum 岸基雷達觀測站內部(Dr. Ziemer)

## 3.4 國際合作可行性討論

本次赴研習GKSS研究中心海岸研究學院之雷達遙測技術研發部，研習近海水文觀測與資料分析技術，除獲得有關雷達遙測原理概念及其如何應用於海洋現象觀測，亦觀摩Dr. Ziemer開發之DiSC模式以及岸基雷達觀測站維護管理作業。其中DiSC模式以及現地雷達觀測站維護管理作業，可爲本署未來發展非接觸式近海水文觀測之參考，故就未來水利署與GKSS研究中心進行國際合作之可行性與Dr.Ziemer討論。

目前GKSS研究中心對於DiSC模式以及岸基雷達觀測系統之輸出，未公開訂定統一價格，僅針對有興趣提出合作之單位進行個案協議。Dr.Ziemer建議可朝國際性之學術研究合作計畫，獲得其主持之雷達遙測技術研發部相關研究成果，並可節省國與國之間訂定協議之時間以及未知之合作經費，故未來水利署可依政府採購法之規定，找尋國內合適之學術研究機構，如大學等，與Dr.Zieme進行國際學術研究之合作，以取得適用於本國近海水文觀測與資料分析之軟硬體相關技術。

# 肆、心得與建議

## 4.1 心得

1. 本次研習近海水文觀測與資料分析技術，除由Dr. Ziemer親自教授雷達觀測原理之概念外，亦觀摩GKSS研究中心之岸基雷達觀測站，瞭解到GKSS研究中心爲理論與實驗操作並重之研究單位。
2. 有關岸基雷達天線開始運作時，雷達資料電腦分析系統與雷達天線之距離，依Dr. Ziemer研究經驗並加以歸納後，應維持於20至50公尺內，以避免觀測資料傳輸發生中斷之情形，並以獲得穩定之資料品質。
3. Dr. Ziemer團隊研發之DiSC模式，係爲分析岸基雷達觀測之影像資料，並從中推衍海流及近岸水深地形等訊息，其使用演算程式語言爲FORTRAN，核心分析技術爲3維快速傅立葉轉換(3-D Fast Fourier Transformation)進行雷達訊號轉換，再應用濾波原理萃取所需資訊後，以2維反快速傅立葉轉換(2-D Inverse Fast Fourier Transformation)產出觀測資料空間分布資訊。該模式經過不斷改良，目前(2009年)已可解析雷達觀測資料之空間解析力至7.5米(2008年時爲40米)，並可推算岸基雷達觀測資料離岸1至2公里範圍內之波浪、流速、水深地形等近海水文參數。
4. 本次研習所觀摩之GKSS研究中心4處岸基雷達觀測站，分別位於德國北部鄰近北海地區之比蘇姆(Büsum)及夕爾特島(Sylt Island)。其中位於比蘇姆(Büsum)及夕爾特島(Sylt Island)南端Rantum之2處岸基雷達觀測站，係採用HF頻段進行觀測，分別另2處係使用X頻段(X-band)進行觀測，皆位於夕爾特島(Sylt Island)北部之利斯特(List)。本次觀摩之4處岸基雷達觀測站，其觀測皆爲應用都卜勒效應(Doppler Effect)，故此4處岸基雷達觀測站，亦稱爲都卜勒雷達系統。
5. 爲節省現地建站經費又可兼顧雷達系統之安全性、機動性以及觀測與維護管理工作之便利性，Dr.Ziemer採用貨櫃屋或拖車配合觀測高塔型式，建立本次觀摩之岸基雷達觀測站。採用貨櫃屋型式者，皆採用HF頻段，其雷達本體建置於貨櫃屋頂部，天線系統(含發射及接收系統)，設置於貨櫃屋旁之岸上，觀測作業所需電力需以電攬外接市電供應；採用脫車配合觀測高塔形式者，係採用X頻段，雷達本體即包含發射及接

收天現系統，觀測作業所需電力由太陽能板及置於拖車內部之發電機供應，其中發電機爲汽油驅動，需於定期維護工作進行時，適時添加油料。無論係採用貨櫃屋或拖車配合觀測高塔型式者，其資料分析系統皆置於屋(車)內，平時採用遠端遙控方式進行觀測作業，如需人員至現場進行觀測與資料分析工作時，可藉由貨櫃屋或拖車金屬外殼之屏蔽效應，保護現地觀測與資料分析人員之安全。

6. 本次研習亦觀察到GKSS所設置之岸基雷達觀測站，需位於當地地形之最高點處，且四周無遮蔽，其中採用HF頻段者，即貨櫃屋型式者，其天線系統(含發射及接收系統)需低於雷達本體。另外，於研習期間和Dr. Ziemer研討時，其表示置於本次觀摩之雷達觀測站內的資訊分析硬體，皆由台灣生產之零組件構成，故台灣如需發展用於近海水文觀測之岸基雷達系統，台灣本身已具有部分生產能力，僅需研發雷達天線本體之硬體設備即可。

## 4.2 建議

1. Dr. Ziemer團隊研發之DiSC模式，係爲分析岸基雷達觀測之影像資料，並從中推衍海流及近岸水深地形資料，目前國內進行與DiSC模式相似之研究尚未成熟，未來可藉由發展國際合作之機會，冀以提昇本國近海水文分析技術。
2. GKSS研究中心所設置之岸基雷達觀測站其維護管理工作，事實上由1人執行即可，但爲安全考量，Dr. Ziemer團隊皆以2人以上進行作業，除可相互照應，確保安全之外，亦可藉由適時之討論，尋找出可提供作業效率之最佳方法。
3. GKSS研究中心位於鄰近漢堡之Schleswig-Holstein州(什列斯威-豪斯敦州，亦有譯爲石勒蘇益格－荷爾斯泰因州，簡稱石－荷州)內的Geesthacht(吉斯哈赫特)之Tesperhude地區，據Dr. Ziemer研究團隊表示，除研究人員外有逾半數的Tesperhude居民係於GKSS研究中心內工作。故GKSS研究中心除了在學術研究上有優異成果外，亦提供地方上的就業機會，對於地方經濟亦有積極之加成效果。或許此例可以提供我國參考，於郊區或商業活動不明顯地區藉由大型研究機構的設立，除了提供研究人員優質的研究環境外、持續蓄積與提昇國家競爭力、以及培

養高素質人力外，同時對於振興地方經濟、提供在地居民就業機會，亦有相得益彰之效果。

# 附錄



# Accuracy of Bathymetric Assessment by Locally Analyzing Radar Ocean Wave Imagery (February 2008)

Stylianos Flampouris, Friedwart Ziemer, and Joerg Seemann

*Abstract*—**In this paper, the error source in assessing the bathymetry by a recently presented method, the dispersive surface classificator, is discussed. This method is based on the analysis of X-band radar image sequences of sea-surface waves to determine spatial maps of hydrographic parameters. To implement this objective, the radar-deduced bathymetry is validating by multibeam echosounder data. The accuracy of the method is high in homogeneous areas and reduced at the areas of bathymetric gradient and lower but comparable with multibeam echosounder data, under the assumption of the spatial resolution. The identification of systematic correlation of the absolute value of the error with the slope is significant and insignificant with the actual depth itself. The spatial correlation of the error illustrates that the direction of the wave field influences the neighboring grid cell in the same direction. The application of the method during crucial weather conditions is the main advantage and permits the accurate operational nearshore monitoring for several applications.**

*Index Terms*—**Area measurement, error analysis, geophysical inverse problems, geophysical measurements, geophysical signal processing, marine radar.**

## I. Introduction

AN ESSENTIAL requirement for a series of coastal and marine activities (coastal research and protection, safe navigation, etc.) is the knowledge of the near shore bathymetry and the current field. The last decades, remote sensing techniques have been broadly used for the imaging of the sea surface to extract those two important physical parameters, as summarized in [1], as state of the art of 2-D observation methods of sea surface.

There are several investigations in the same subject in which digital video images were inverted to define the bathymetry [2]–[4] and to infrared imagery of near shore shoaling waves [5], [6]; the expansion of the methods is applicable to the coastline problems management [7].

These investigating efforts are based among few pioneer publications, such as [8] and [9] who had measured the surface current field by using time sequential imagery to determine the change in the frequency-wavenumber dispersion relation by using X-band radars.

The assumptions in this investigation for the modeling of the sea surface gravitational waves are that the fluid is incompressible and the motion is irrotational, in mathematical terms those assumptions are expressed by the partial differential equation known as Laplace. The solution of the Laplace equation under the boundary conditions of the specification of the bottom, the kinematic surface and the free surface, is linear and periodic in space and time propagating over a horizontal surface. The linear dispersion relation in shallow water is expressed as function of the depth $d$ and the surface current vector $\vec{u}_c$

$$\widetilde{\omega}(\vec{k}) = \pm\sqrt{|\vec{g}\cdot\vec{k}|\tanh\left(|\vec{k}|d\right)} + (\vec{k}\cdot\vec{u}_c) \qquad (1)$$

where $\widetilde{\omega}$ is the radial frequency, $\vec{k}$ the wavenumber, $d$ the depth, $\vec{u}_c$ the current velocity, and $\vec{g}$ the gravitational acceleration.

During the last two decades, several scientific research results have been published about the retrieval of the bathymetry by inverse modeling the linear wave dispersion [10]–[13]. The method used in those publications, here called the "global method," is based on the analysis of radar intensity variance spectra calculated by the squared modulus of a 3-D fast Fourier transformation performed on the full size image sequences, the 3-D FFT in terms of image processing is a global operator. Since 2000, a series of investigations in the localization of the wave energy and the inverse in local scale for the determination of the local depth and current vector, have been published [14]–[16]; in 2007, an alternative method which combines the advantages of the previous investigations was presented [17].

The method analyzes image sequences of dynamic dispersive boundaries, utilized to determine physical parameters on a local spatial scale. The local analysis method, which allows the analysis of inhomogeneous image sequences of a dynamic and dispersive surface, has been labeled dispersive surface classificator (DiSC). The main advantage of the method is the extraction of the bathymetry and the current field, which is deduced by the 3-D spectrum component of the observed area, in long integration time (up to 10 min) and high spatial resolution (40 m × 40 m). The statistical significance of the result is high in comparison to the rest of the methods as a set of full waves spectrum is analyzed and not only one wave component.

Manuscript received October 1, 2007; revised December 19, 2007. Current version published October 1, 2008. This work was supported by in part by the EUFP5 project ORCIMA EVK3-CT-2001-00053.

S. Flampouris and F. Ziemer are with GKSS Research Center, 21502 Geesthacht, Germany (e-mail: stylianos.flampouris@gkss.de; friedwart.ziemer@gkss.de).

J. Seemann is with the V2T VISION TO TECHNOLOGY GmbH, 21502 Geesthacht, Germany (e-mail: seemann@v2t.de).

Digital Object Identifier 10.1109/TGRS.2008.919687

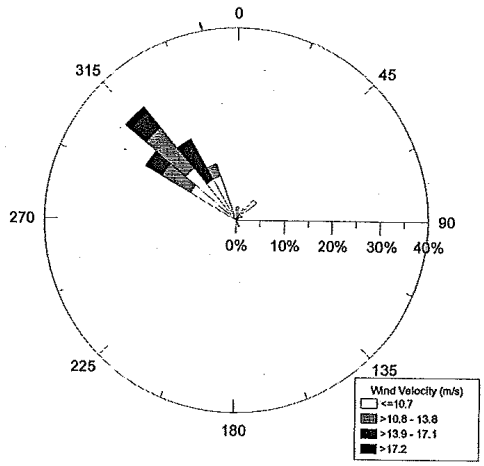


Fig. 1. Wind plot for 50 h before and during the acquisition of the radar data, the data have been acquired, every 6 s, by the meteorological station mounted on the radar mast and has been averaged up to 10 min.

This investigation mainly concerns the impact of the current and wave regime on the sea bottom morphology in shallow water regions with nonconsolidated sediment during crucial weather conditions and the extend discussion of the error in DiSC-deduced bathymetry by comparing it with multibeam echo sounding data.

It is evident that the applicability of the DiSC depends on the wave conditions, as the method requires waves, long enough, to be influenced by the sea bottom. In [3] and [13], it is proved that in moderate wave heights the correct depth is retrieved. However, the increase of the rms wave height from 1 to 3.5 m produced much poorer depth estimation, which indicates that neglecting the amplitude dispersion effect would result an overestimation of water depth. In practice, in the area of research that this investigation focuses, the maximum observed wave heights did not exceed 2 m [18], [19]. The minimum in meteorological conditions during the observation should be 5-in Beaufort scale so that the backscatter energy is significant and the wavefield is long enough to carry the bathymetric information. In this paper, the DiSC method is applied to a data set collected over 12-h time period, between 26th of August 2003, 23.00 and 27th of August 2003, 10.00. The wind conditions for more than 36 h before the data acquisition were constantly from the northwest (Fig. 1) stronger than 8 m/s and were increasing up to 18 m/s during the sampling (Fig. 2). At the same period, the significant wave height was varying between 1.2 and 1.7 m, and the tide had a normal period of 12.3 h and approximately 2-m range (Fig. 3).

For the complete approach of the subject, the present publication is divided into four main paragraphs. The first one is the description of the region of investigation. In the second paragraph, the acquired data are summarized and the next paragraph describes the core of the DiSC and the other algorithms that were used for the data analysis. In the third paragraph, the results of the investigation are presented and in the last paragraph, the error of the method is discussed.

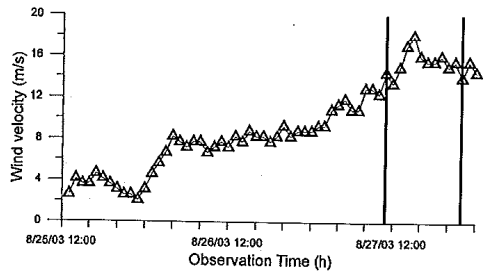


Fig. 2. Time series of the wind magnitude for 50 h before and during the radar observations, the period of radar observation is indicated by the two perpendicular solid lines, the wind magnitude is the first 10-min average of each hour.

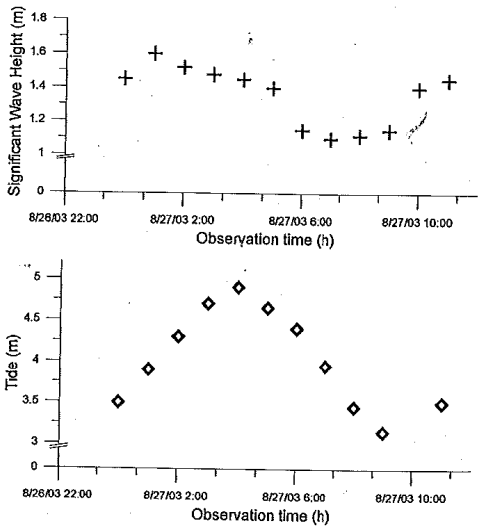


Fig. 3. (Top) Significant wave height observation by wave rider in the area of radar range, during the radar data acquisition. (Bottom) Tide signal from the pile of Hornuem, 18 nm southern, lag transferred model has been applied.

## II. Area of Investigation

The area of research is the West List, northwest side of the Sylt Island, laying in the German Bight. The Island of Sylt is located on the West coast of Schleswig-Holstein at the North Sea coast of Germany, and it is the most northern sandy barrier island of the Frisian chain of the North Sea coast, Fig. 4. It has a length of 35 km and a width up to 13 km, its surface is 99 km$^2$, [20]. There are several scientific, economical, and social criteria for the choice of this specific area.

Since the half of the 20th century, several different methods have been used for the encounter of the high and rapid erosion of the west coasts of the island, the beach nourishment has been proved the most effective [20]. The island started getting the current shape about the 17th century and in general the northern and southern spit, is under continuous change. The tide, in area of Sylt is semidiurnal and the tidal ranges reach approximately

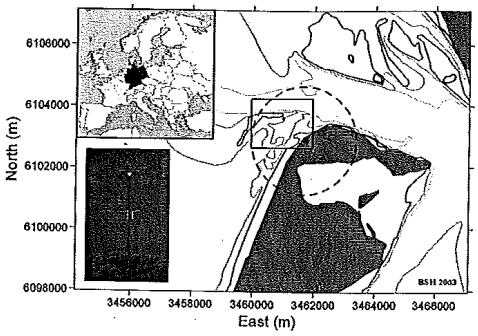


Fig. 4. Experimental site Sylt (lighthouse List West), clock wise starting by the top left map, the dot on the map of Europe localize the Sylt Island in North Sea, at the borders of Germany with Denmark. The main figure represents the depth isolines of the monitored area, the radar is indicated by the black dot, the radar range is indicated by the dashed line, the orthogonal indicates the area of results (see Fig. 6) (sea-map source: Bundesamt fuer Seeschiffahrt und Hydrographie). The blue dot indicates the wave rider position. The photography shows the radar mast on which a Furuno radar and the meteorological station are mounted.

2 m, which causes cross shore transport through the channels between barrier islands. The long shore transport along the coast is mainly wave-induced and, therefore, also alternates in direction, this is obvious at Sylt.

Tidal currents are dominant seaward of the longshore bar, with resulting sediment transport to the north. It is proved by measurements of sediment transport that the coast is eroding along the entire western coast and that the net long shore transport is directed northward at the northern part of Sylt [21]. More precisely, in the southern area covered by the radar range, there is regular beach nourishment, approximately every second year; the human-deposited sediment migrates to the northern eastern part of the island or to the neighboring Rømo Isle. The island loses the majority of this sand through storm surges, it is observed that an eight-day storm is responsible for the transportation of 50.000 $m^3$ in an area of 12 $km^2$ [22]. In general, the synergy of the waves and tides continuously erode and move away material from the sandy shore and foreshore area, causing structural erosion.

## III. Data Acquisition

The X-band radar was mounted close to the List West Light house at Sylt Isle. The area covered by the radar images shows the List West, the Lister Landtief, and parts of the Lister Tief. The used instrument for the acquisition of the sea surface is a software–hardware combination, presented by [23] as part of the wave monitoring system (WaMoS), consisting of a Furuno FR 1201 [24] nautical radar, a WaMoS II analog–digital converter, and a WaMoS II software package for the acquisition of the radar images. The used instrument for the observation is a ground-based nautical X-band radar with horizontal polarization, mounted 25 m above the NN. The radar was mounted for about six years; the period of the present investigation, the image sequences were recorded hourly from 23:00 UTC on 26.08.2003 to 10:00 UTC on 27.08.2003, during the radar data acquisition.

The bed relief of the surveyed area was mapped by coupling multibeam survey technique with high accuracy positioning. Bed survey was carried out by means of the multibeam echosounder EM 3000 from Simrad–Kongsberg. This system is designed to work in water depths from 3 to 200 m, it operates at a frequency of 300 kHz with a ping repetition rate of 15 Hz. The nominal apex angle is 1.5° along-track and 120° across-track during transmission, and 30° along-track and 1.5° across-track during receiving. This result in an array of 127 individual beams with an effective 1.5° × 1.5° apex angle per single beam arranged with some overlap over an arc of 120° [25]. The 3-D sonar head positions and orientations were finally fixed by combining antenna position (Trimble 4000 ssi), gyrocompass (Anschütz 20, 4) and motion sensor (DMS-05, TSS UK LTD) data. The ship position accuracy is on the order of centimeters, and the relative positions of all components onboard the ship were measured with accuracy of millimeters. The data for the present investigation were acquired in August 25, 2003.

The Directional Waverider Mark II is a spherical, 0.9-m diameter, buoy which measures wave height and wave direction. The direction measurement is based on the translational principle which means that horizontal motions instead of wave slopes are measured. As a consequence the measurement is independent on buoy roll motions and, therefore, a relative small spherical buoy can be used. A single point vertical mooring ensures sufficient symmetrical horizontal buoy response also for small motions at low frequencies. The buoy is moored on 55° 03, 26 N 08° 23, 42 E.

The tide data were acquired at the hydrographic pile in Hoernum of Sylt Isle, which is in operation since 2002, and acquires hydrographic and meteorological measurements within the Wadden Sea.

The weather parameters were measured by the Meteorological Weather Station manufactured by Siggelkow Geraetbau GmbH [26] mounted on the radar mast, approximately 23 m above NN. The monitored parameters are the minimum, maximum, and 10-min mean of wind magnitude and direction.

## IV. Analysis Method

### A. DiSC

The local changes of the wave field, containing information on the local bathymetry information and the shearing currents are inverted. To increase the accuracy of the result, waves with high distribution in frequency and direction are required.

The DiSC has been presented in [17]; the method requires stationarity and inhomogeneity of the wavefield, in contrast with any global method that requires homogeneity. The steps of the method are shown in Fig. 5, the following brief description, which analyzes image sequences of oscillations at dynamic dispersive boundaries and used to determine physical parameters on a spatial grid.

The DiSC is a multistep method; the radar data system acquisition yields image sequences in polar coordinates preservation of the complex-valued 3-D FFT image spectrum, for the minimization of the computational time the discrete raw-image sequences are transformed to image sequences given in Cartesian coordinates. The first step of the algorithm is the transformation of the image sequence to the spectral domain by 3-D FFT. By using filtering techniques, the complex-valued

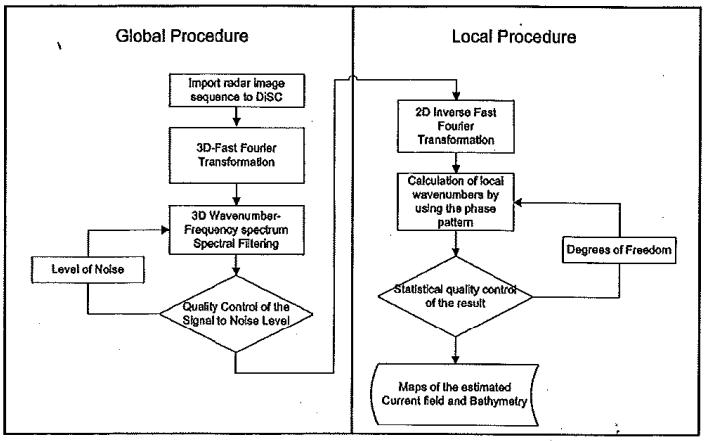


Fig. 5. Scheme of the procedural and data flow of DiSC. The relation between the continuous spatiotemporal sea-surface elevation and nautical radar image sequence is described by an image transfer function. The image sequence acquisition system yields image sequences in polar coordinates, but the discrete raw-image sequences are transformed to image sequences given in Cartesian coordinates. To retrieve global hydrographic parameters the global analysis is performed on the discrete 3-D gray-level variance spectra of the image sequence. For spatial hydrographic parameter maps, the local method DiSC is performed on discrete complex-valued 3-D spectra where by the phase information the spatial structure of the images sequences is preserved.

image spectrum is decomposed and the wave signal is separated from the noise and simultaneously the direction and the dispersion of the complex-valued spectrum is separated into spectral bins at 2-D wavenumber planes of constant frequencies. The next step is the 2-D inverse fast Fourier transformation (2-D $\mathrm{FFT}^{-1}$) of the spectral bins, yielding complex-valued, to one-component spatial maps in the spatiofrequency domain, which are used for the calculation of spatial maps of local wavenumbers from the one-component images of constant frequency. The resulting one-component local wavenumber are composed to maps of constant frequency to local 3-D spectra and finally by using the spatial maps of local wavenumber vectors and power for the calculation of spatial hydrographic-parameter maps. The number of the local wavenumbers from the one-component images is counted and is used as criterion for the results significancy [18].

The method was applied in a 12-h data set of radar images. For increasing the degrees of freedom, all DiSC maps of the tidal cycle were averaged, as they could be assumed to be statistical independent measurements. The spatial resolution of the DiSC result is approximately 40 m × 40 m (corresponding to 6 pixel × 6 pixel), Table I. For the determination of common reference level, the sea level measurements in Hoernum are extrapolated by a model into experimental site (see Section IV-C).

### B. Multibeam Echosounder Data

The multibeam echosounder measurements were further processed in a digital terrain model (DTM). The DTM employed used the "Seabed" algorithm [27]. In this method, for each grid node a surface paraboloid is computed from a weighted fit through all data points within a user-definable search radius. The altitude of each DTM cell is defined by the value of the parabolic surface at the grid node point. The grid size of the terrain model is 2 m × 2 m. All results shown in the following are based on this DTM and each grid cell contain 25 to 50 data points.

TABLE I
SPECIFICATION OF THE CARTESIAN GRID OF THE NAUTICAL RADAR IMAGE SEQUENCES

| | |
|---|---|
| Number of pixel in x–direction(west–east) Nx | 576 |
| Cartesian-grid pixel resolution in x–direction (west–east) Δx | 6.82 m |
| Spatial length in x–direction (west–east) X | 3928 m |
| Number of pixel in y–direction (south–north) Ny | 576 |
| Cartesian-grid pixel resolution in y–direction(south–north)Δy | 6.82 m |
| Spatial length in x–direction (south–north)Y | 3928 m |
| Number of images per image sequence Nt | 256 |
| Temporal resolution (antenna-rotation time) Δt | 1.77 s |
| Temporal length of an image sequence T | 453 s |

The multibeam echosounder data were acquired on 25.08.2003 and the spatial grid cell resolution of the data is 2 m × 2 m; for the comparison with the DiSC results, the echosoundings have been averaged spatially in the radar grid with resolution 40 m × 40 m, at the same coordinates.

### C. Tidal Model

For the determination of a common reference level, a combination of tidal prediction model and sea level measurements was used. The used model is a simplified version of the XTide Copyright 1998 [28], which is provided under the terms of the GNU General Public License. The model summarizes the cosine functions, for which the tidal harmonics distributed by the NOAA National Ocean Service have to be imported. For the minimization of the deviation of the surface wind friction, the synchronous measurements of the tide level are taken into account, under the assumption that the wind influence on the sea level along the west coast of Sylt Isle is homogeneous.

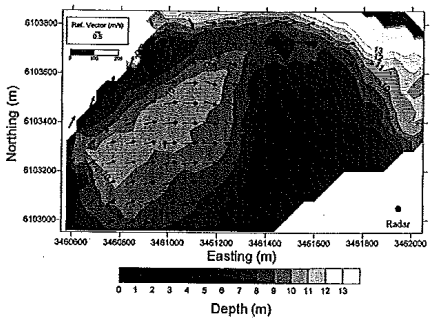


Fig. 6. Results of DiSC on August 27, 2003 at 03.00 UTC, isolines of the instantaneous bathymetry and the current field during the flooding.

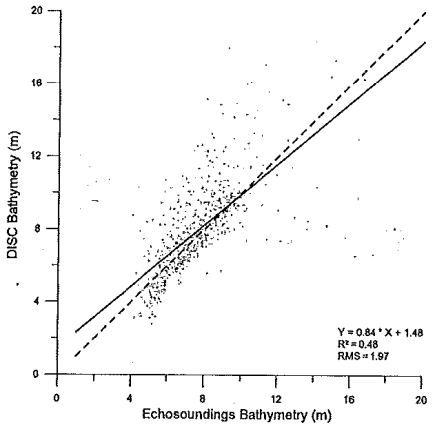


Fig. 7. Multibeam echosounder bathymetry versus DiSC-deduced bathymetry. The regression line is a straight line fit across the data, and it is estimated by least squares fit. The dashed line is the $y = x$ line.

## V. Results

Hourly bathymetric maps, with grid cell resolution 40 m × 40 m, have been produced for the period of a tidal cycle, 12 h. The current field observation as necessary coproduct of the analysis is overlapped and shown in Fig. 6 for the flooding at 27.08.2003 at 03:00 UTC. To increase the significance of the result, the 12 maps were averaged. To define a common reference level between the average DiSC bathymetry and the echosounder one, tide gauge correction was applied.

The averaged bathymetric values of the DiSC show insignificant correlation with the echosounder bathymetry, even thought that the main part of them present one-to-one linear trend (Fig. 7). The uncorrelated data consist two clusters; the first one is a systematic overestimation of the depth by DiSC across the whole data set, the second cluster is the underestimation of the bathymetry in the deep than 12-m areas. About the main part of the data, the data are markedly offset toward shallower radar retrieval in shallow area for depths less than 6 m.

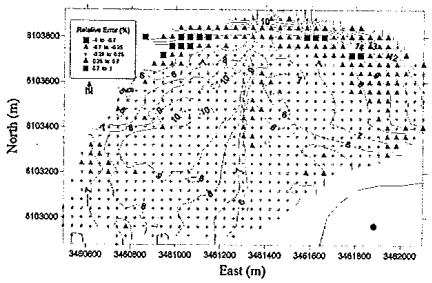


Fig. 8. Overlay of the multibeam echosounder bathymetry (isolines) with the relative error of the DiSC-deduced bathymetry; the orange color is used for the negative (overestimation) values, and the black for the positive (underestimation).

The spatial plot of the error illustrates its spatial clustering. For this reason, the relative error is plotted over the actual bathymetry surveyed by the multibeam echosounder, Fig. 8. The crosses illustrate error under the accuracy of the method as it is presented in [17].

The circles indicate the error of ±25%. The gray color indicates negative error (overestimation of the depth) in opposite the black color indicates positive error (underestimation of the depth), in both cases the triangles indicate error between 25% and 70% and the squares indicate error between 70% and 100%. The general comment about the error spatial distribution is that the error depends on the distance from the radar.

More specific, in the northeast side, deep ($d > 12$ m) area the error is positive and up to 70%. In the deeper parts, the wavelength is smaller than the depth, therefore the error increases as function of depth, but it is not possible to identify the mathematical relation, because of the high variability of the error. The highest values of the error occur over the grid cells with high bathymetric gradient. By using the absolute relative error, the data were separated into groups with step width of 0.05. The plot of the mean value of the relative error of each group versus the mean value of the sea bottom, as deducted by DiSC, proves correlation between those two parameters (Fig. 9). As the main error source identified the influence of the bottom slope on the wavefield, the question is about the error propagation in between the grid cells. The spatial correlation of the error (Fig. 10) shows that the error of the depth in each grid cell has significant correlation only with one neighboring grid cell. The disclosure of the correlation is the nonsignificant spatial correlated error has the same direction as the propagating wavefield.

The previously mentioned observations forced for the development of a method for the determination of the significance of the DiSC results and the filtering out of nonsignificant results. By using the number of the fitting wave components, which influences the significance of the results, and compiling the knowledge that the error is not propagating within the grid, each grid cell bathymetry has been filtered; the minimum of regression points is defined: 30. In addition, a second filter has been applied; the second filter is arranged according to the bathymetric gradient, the grid cells having DiSC-deduced slope above 2°, have been filtered out. The remaining averaged bathymetric values of the DiSC have been plotted against the

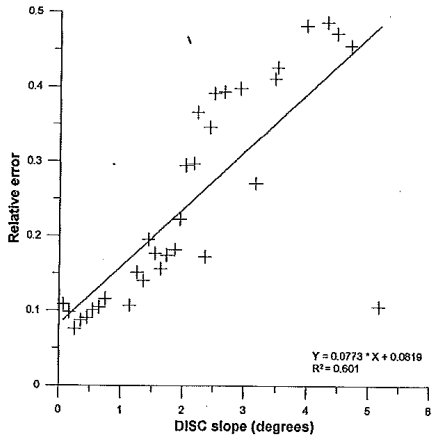


Fig. 9. Scatter plot of the relative error versus the sea bottom slope, as it is estimated by DiSC.

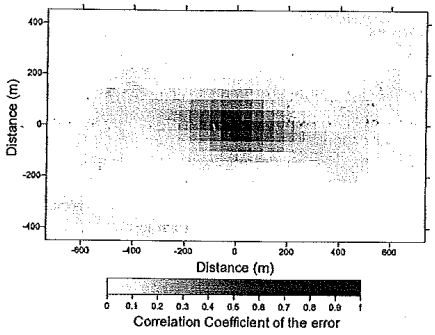


Fig. 10. Spatial correlation of the relative error.

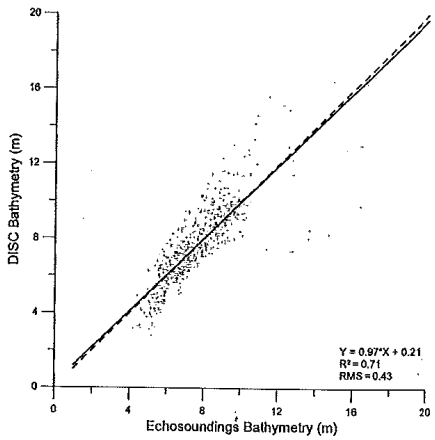


Fig. 11. Multibeam echosounder bathymetry versus DiSC-deduced bathymetry, after the identification of the error sources. The regression line is a straight line fit across the data, and it is estimated by least squares fit. The dashed line is the $y = x$ line.

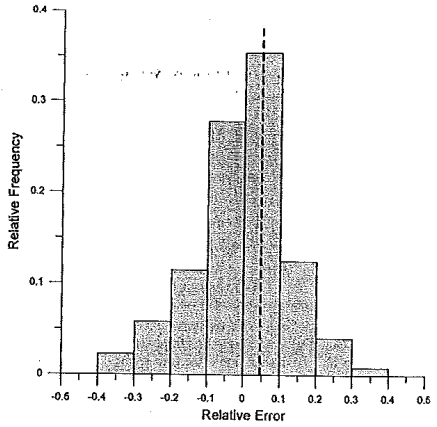


Fig. 12. Relative error distribution, the error of more than 80% of the grid cells is less than 20%. The dashed line indicates the mean error of all the grid cells.

echosounder data (Fig. 11); the main characteristics are similar with the scatter plot in Fig. 7, except the minimization of the scatter. The frequency distribution of the relative error (Fig. 12) and the mean value proves a systematic underestimation of depth by DiSC approximately 5%.

## VI. Discussion

The validation of the DiSC over the optimal meteorological and wave conditions confirms the validity of using the finite dispersion relation for depth deduction in nearshore areas.

The hourly results of the bathymetry and the current field (Fig. 6) give a first assessment of the instantaneous depth and current. In previous investigations [29], it was proved that the bias in the hourly results is approximately 0.4 m. For the increase of the depth results significance the bathymetry is calculated over a tidal cycle in this approach.

The general impression is that the DiSC overestimates the bathymetry about 10%. The precision of 80% of the DiSC results is lower but comparable with high-resolution multibeam echo sounding coupled with high-accuracy positioning, [30], considering the spatial resolution of the two methods and the coverage density of the two systems. The main error source is the changing in the bathymetric gradient, but the error is not propagating along the grid.

The frequency distribution of the bias of the depth estimation is shown in Fig. 12, the mean error is less than 10%; the DiSC overestimates the depth. The most probable physical reason for the error that appears on the highest point of the slope is the impact of the slope itself on the waves, by approaching shallow areas, the impact of the seafloor and the bathymetric gradient transform the geometry of the waves, shoaling. The wave crests become steeper, the wave height increases, shifting the maximum of the radar return toward the crest, which influences the imaging of the wavefield and causes the overestimation of the depth.

In addition, to the physical phenomenon, the transfer function should be considered as an error source. The spatial distribution of the error proved a strong relation between the error and the distance from the radar. For the whole monitored area, the same transfer function is used for transformation of the received energy to sea wave energy, this assumption is strong enough and broadly used in many different radar systems (WaMoS [31], Miros [32]), but due to the high resolution of the monitored geological structures and mainly their orientation toward the radar beams and the influence to the wavefield, it has probably an important impact.

More precisely, Figs. 7 and 11 show that in shallow areas, nominally less than 4 m, the DiSC does not produce results, during the specific conditions, the wavefield is strongly nonlinear, as the waves are breaking due to the shoaling; therefore, the applied linear physical model fails to model the actual wave conditions and its inversion is impossible. As the method is based on the linear wave theory, by assuming the depth ($d$) comparable small to wavelength ($\lambda$) and the $\vec{u}_c = 0$, the dispersion relation (1) is transformed into $\bar{\omega}(\vec{k}) = \sqrt{|\vec{g}|d}$, which is the lower limit of the method. In the practice, the lower limit of the method depends on the radar resolution, in this case 7 m, therefore the shortest observed waves have approximately 28 m length. In the scatter plots, it is obvious that the DiSC underestimates the depth between, approximately, 4 and 6 m; this is due to the first, weak, impact of the shoaling, which by itself is a nonlinear phenomenon, of the waves approaching the shore.

The majority of DiSC-deduced bathymetry between 6 and 10 m, presents significant correspondence with the echo sounder data, the accuracy is higher than 90%, the result is similar with the field observations of [3]. The main source of error is the systematic underestimation of the depth, which exceeds in few case 40% and it is obvious as a cloud of regression points parallel to the fit line. The geocodation of the results and the overlapping with the multibeam bathymetry, Fig. 8 show that the underestimation is caused mainly at the deep areas where the waves are too short to be influenced by the bathymetry, DiSC underestimates, approximately, the 90% of areas deeper than 11 m. The few available depth grid cells do not permit to make general statements about the error source, under the specific wave conditions during the data acquisition and the geomorphology of the area, the decrease of the accuracy seems reasonable. The upper limit of the method range depends on the wave conditions. For the determination of theoretical limit, assuming that $d \gg \lambda$, so $\tanh(|\vec{k}|d) \approx 1$ holds, substituted in the dispersion relation (1) $\bar{\omega}(\vec{k}) = \sqrt{\vec{g} \cdot \vec{k}}$, independent to the depth; therefore, the result of the inversion is ambiguous. In this case, the upper limit of the method is approximately 15-m depth, but the distance from the radar and the low backscattered energy is the practical limitation.

The scatter plot (Fig. 9) of the absolute relative error versus the bathymetric gradient, as it is calculated from the DiSC results, indicates a significant correlation between those two quantities. The error presents two main clusters and one outlier as function of the slope, the first cluster lies between 0° and 2° and the second cluster lies between 2° and 6°; in addition, the difference between the two clusters is a constant offset of 0.1. The geocodation of the error (Fig. 9) shows that the high error is coming from the areas with high seafloor gradient, mainly at the shallow borders of the traffic channel. The erroneous results are presented at the areas with high gradient and one neighboring grid cell. The strongest indicating example that the error depends on the bottom slope, lies approximately among [(6103200, 3461200), (6103500, 3461350)], where the error is doubled in comparison with the neighboring grid cells.

The spatial autocorrelation of the error (Fig. 10) proved that the error does not propagated into the grid, therefore each bathymetric result for individual grid cell is considered as independent measurement. The benefit is the use of statistics for the exclusion of the insignificant DiSC bathymetric results.

## VII. Conclusion

The last decades, several efforts about the determination of the bathymetry by inverse modeling the wave propagation, approached by linear or nonlinear models have been published. However, in few of them, there is an extensive validation and discussion about the error. The DiSC should be considered a state-of-the-art method for the bathymetric monitoring of the coastal areas; as it is proved the significant accuracy and it has high temporal and spatial resolution.

In the homogeneous areas where there is not high variation in the bathymetry (slope less than 2°), the error is approximately 7%. In comparison with the multibeam echosoundings data, the radar-deduced bathymetry has similar accuracy under the assumption of a common grid cell. At the areas with high bathymetric variability, the error is about 40%. The two main sources of error are the high bathymetric gradient (slope steeper than 2°), which influence the geometry of the waves, and the linear wave dispersion, which is no longer applicable when the wavelength is too small to be influenced by the seafloor. The error is strongly correlated with the slope, which has the main nonlinear impact on the waves. The error each grid cell is significantly correlated with a neighboring grid cell in the direction of the wavefield.

In general, the DiSC method is an alternative remote-sensing method for coastal water monitoring, which has satisfactory and comparable accuracy with *in situ* measurements, like echosoundings, and it is applicable in areas of high interest where it is essential to constantly monitor with high resolution in time. The disadvantages of the *in situ* techniques are the high expenses due to long shipping times necessary to retrieve the required information. As a consequence, the temporal evolution of morphodynamically highly active areas is not possible during strong breeze or heavier weather conditions. To overcome this problem, the DiSC technique, based on the analysis of nautical X-band radar image sequences of the sea-surface waves, could be used.

The current level of method permits the operational application in areas for important activities, such as, ship navigation, tracking sediment movement and for model validation and for data assimilation in real-time forecasting, as the inversion of the above conclusions and the knowledge of the error sources permit the production of the confidence maps of the DiSC bathymetry.

## Acknowledgment

The authors would like to thank all the scientific companions of Radar Hydrography Department of GKSS for the harmonic

corporation and the discussions about each of the occurred problems during the analytical process and particularly to G. Schymura for his dedication to the radar systems to provide continuous and high-quality data. The multibeam data have been provided by Dr. R. Riethmuller and M. Heinecke (GKSS Research Center). Finally, the authors would also like to thank Dr. C. Senet (V2T VISION TO TECHNOLOGY) for sharing his experience with DiSC.

## REFERENCES

[1] A. Lane, P. J. Knight, and R. Player, "Current measurement technology for near-shore waters," *Coast. Eng.*, vol. 37, no. 3, pp. 343–368, Aug. 1999.

[2] H. F. Stockdon and R. A. Holman, "Estimation of wave phase speed and nearshore bathymetry from video imagery," *J. Geophys. Res.*, vol. 105, no. C9, pp. 22 015–22 034, Sep. 2000.

[3] K. Holland, "Application of the linear dispersion relation with respect to depth inversion and remotely sensed imagery," *IEEE Trans. Geosci. Remote Sens.*, vol. 39, no. 9, pp. 2060–2072, Sep. 2001.

[4] S. Misra, A. Kennedy, and J. Kirby, "An approach to determining nearshore bathymetry using remotely sensed ocean surface dynamics," *Coast. Eng.*, vol. 47, no. 3, pp. 265–293, Jan. 2003.

[5] J. P. Dugan, H. H. Suzukawa, C. P. Forsythe, and M. S. Farber, "Ocean wave dispersion surface measured with airborne IR imaging system," *IEEE Trans. Geosci. Remote Sens.*, vol. 34, no. 5, pp. 1282–1284, Sep. 1996.

[6] J. P. Dugan, C. P. Forsythe, H. H. Suzukawa, and M. S. Farber, "Bathymetry estimates from long range airborne imaging systems," in *Proc. 4th Int. Conf. Remote Sens. Marine Coastal Environ.*, Orlando, FL, 1997.

[7] A. Kroon, M. A. Davidson, S. G. J. Aarninkhof, R. Archetti, C. Armaroli, M. Gonzalez, S. Medri, A. Osorio, T. Aagaard, R. A. Holman, and R. Spanhoff, "Application of remote sensing video systems to coastline management problems," *Coast. Eng.*, vol. 54, no. 6/7, pp. 493–505, Jun./Jul. 2007.

[8] I. Young, W. Rosenthal, and F. Ziemer, "A three-dimensional analysis of marine radar images for the determination of ocean wave directionality and surface currents," *J. Geophys. Res.*, vol. 90, no. C1, pp. 1049–1059, 1985.

[9] F. Ziemer, "Directional spectra from shipboard navigational radar during Lewex," in *Directional Ocean Wave Spectra*. Baltimore, MD: The Johns Hopkins Univ. Press, 1989.

[10] C. M. Senet, J. Seemann, and F. Ziemer, "An iterative technique to determine the near surface current velocity from time series of sea surface images," in *Proc. Oceans*, Halifax, NS, Canada, 1997, pp. 66–72.

[11] P. Bell, "Shallow water bathymetry derived from an analysis of X-band marine radar images of waves," *Coast. Eng.*, vol. 37, no. 3/4, pp. 513–527, Aug. 1999.

[12] K. Hessner, K. Reichert, and W. Rosenthal, "Mapping of sea bottom topography in shallow seas by using a nautical radar," in *Proc. 2nd Int. Symp. Operationalization Remote Sens.*, 1999. CD-ROM.

[13] D. Trizna, "Errors in bathymetric retrievals using linear dispersion in 3D FFT analysis of marine radar ocean wave imagery," *IEEE Trans. Geosci. Remote Sens.*, vol. 39, no. 11, pp. 2465–2469, Nov. 2001.

[14] C. Senet, J. Seemann, and F. Ziemer, "Dispersive surface classification: Local analysis of optical image sequences of the water surface to determine hydrographics parameter maps," in *Proc. Oceans MTS/IEEE Conf.*, 2000. CD-ROM.

[15] C. Senet, J. Seemann, G. Schymura, and F. Ziemer, "Verfahren und Vorrichtung zur Ermittlung von ein Seegangsfeld in einem Wellentank beschreibenden hydrographischen Parametern," German patent Office, Munich, Germany, in German, German and international patent application, Ref. 100 35 931.0 (German Patent Application), Ref. PCT/DE 00/02413 (international patent application), 2000.

[16] J. Seemann, C. Senet, and F. Ziemer, "Verfahren zur Ermittlung von ein in situ Seegangsfeld beschreibenden hydrographischen Parametern mittels einer Radareinrichtung," German patent office, Munich, Germany, in German, German and international patent application, Ref. 100 35 921.3 (German patent application), Ref. PCT/DE 00/02413 (international patent application), 2000.

[17] C. Senet, J. Seemann, S. Flampouris, and F. Ziemer, "Determination of bathymetric and current maps by the method DiSC based on the analysis of nautical X-band radar-image sequences of the sea surface," *IEEE Trans. Geosci. Remote Sens.*, vol. 46, no. 7, Jul. 2008.

[18] S. Flampouris, "Investigation of correlations between radar deduced bathymetries due to the outer impact of a storm in the area Salzsand," M.S. thesis, GKSS, Geesthacht, Germany, 2006.

[19] M. Chowdhury, *Assessment of Water Flow and the Impact on Sediment Motion in a Tidal Channel of North Sylt Basing on Radar Observation*. Kiel, Gemany: Coastal Res. Lab., Christian Albrecht Univ. Kiel, 2007.

[20] P. Doddy, M. Ferreria, S. Lombardo, I. Luicas, R. Misdorp, H. Niesing, A. Salman, and M. Smallegange, *Living With Coastal Erosion in Europe—Sediment and Space for Sustainability, Results From the Eurosion Study*. Luxembourg, U.K.: Eur. Commission Publication, 2004.

[21] P. Sistermans and O. Nieuwenhuis, *Isle of Sylt: Isles Schleswig-Holstein (Germany)—A Case Study of European Initiative for Sustainable Coastal Erosion Management (Eurosion)*, 2004, Amersfoort, The Netherlands.

[22] S. Flampouris and F. Ziemer, "Comparison of bathymetric changes observed by radar on different time scales," in *Proc. SeaTech Week*, Brest, France, 2006.

[23] J. C. N. Borge, K. Reichert, and J. Dittmer, "Use of nautical radar as a wave monitoring instrument," *Coast. Eng.*, vol. 37, no. 3/4, pp. 331–342, Aug. 1999.

[24] Anonymous, *FURUNO—Operators Manuals for FR 1201*, 1989, Nishinomiya, Japan: Furuno Electric Co. Ltd.

[25] K. Stockmann, R. Riethmüller, M. Heinecke, and G. Gayer, "On the morphological long-term development of dumped material in a low-energetic environment close to the German Baltic coast," *J. Mar. Syst.*, 2006, to be published.

[26] Anonymous, *Meßsysteme für Meteorologie und Umweltschutz*, 2000, Hamburg, Germany: Siggelkow Gerätebau GmbH.

[27] *"Seabed" Algorithm*, Roxar Software Solutions AS, Oslo, Norway, 2003. Cfloor Version 6.2.2, Users Guide.

[28] D. Flater, *XTide*, 1998. [Online]. Available: http://www.flaterco.com/

[29] C. M. Senet and J. Seemann, "Studie II: 'Validation'," GKSS Res. Center GmbH, Geesthacht, Germany, 2002. Tech. Rep.

[30] V. Ernstsen, R. Noormets, D. Hebbeln, A. Bartholomä, and B. Flemming, "Precision of high-resolution multibeam echo sounding coupled with high-accuracy positioning in a shallow water coastal environment," *Geo Mar. Lett.*, vol. 26, no. 3, pp. 141–149, Sep. 2006.

[31] J. C. Nieto, K. Reichert, J. Dittmer, and W. Rosenthal, "WaMoS II: A wave and current monitoring system," in *Proc. COST 714 Conf. Directional Wave Spectra*, Paris, France, 1998.

[32] Ø. Gepnlie, *Wave Radars—A Comparism of Concepts and Techniques*. Portland, ME: Hydro Int., 2006.

**Stylianos Flampouris** received the first degree in marine sciences from the University of the Aegean, Mytilene, Greece, in 2003, the M.Sc. degree in mathematical modeling in physical sciences and new technologies from the University of the Aegean, Karlovasi, Greece, in 2004, and the M.Sc. degree in coastal geosciences and engineering from Christians-Albrechts Universität zu Kiel, Kiel, Germany, in 2006. Since 2006, he has been working toward the Ph.D. degree at the GKSS Research Center, Geesthacht, Germany.

**Friedwart Ziemer** received the Ph.D. degree in geosciences from the University of Hamburg, Hamburg, Germany.

He is currently with the GKSS Research Center, Geesthacht, Germany. He has many years of experience in marine data acquisition for the validation of remote sensing and model results. He is the author or coauthor of more than 40 scientific publications. He participates in three patents in connection with the extraction of hydrodynamic parameter values from radar image series. He has coordinated the EU projects HYMNE and OROMA, and he has been a partner in several national and international projects.

**Joerg Seemann** received the Diploma degree in physics and the Ph.D. degree in geosciences from the University of Hamburg, Hamburg, Germany, in 1993 and 1997, respectively.

Since 2001, he has been the Head of the V2T VISION TO TECHNOLOGY GmbH, Geesthacht, Germany, where he is responsible for the software engineering of machine vision systems. His research interests as a scientist have been laser spectroscopy and oceanic and coastal radar remote sensing.

IGARSS 2009

# Observing Littoral waves by Doppler radar

*Stylianos Flampouris, Joerg Seemann, Friedwart Ziemer*

GKSS, Max Planck Str. 1, D-21502 Geesthacht, Germany;
stylianos.flampouris@gkss.de; joerg.seemann@gkss.de; friedwart.ziemer@gkss.de

## ABSTRACT

The offshore observation of the wavefield with coherent radar systems consist a common practice for the study of the electromagnetic waves probing the sea surface waves and for the extraction of information of the sea waves. In this investigation, a Dopplerized, horizontally polarized, nautical radar is utilized for the monitoring of the wavefield evolution in the littoral zone. The radar datasets are globally unique and cover different geophysical conditions; therefore the impact of the bathymetry on the Doppler spectra is discussed, the horizontal velocity towards the shore is calculated and the properties of the radar deduced quantities are compared with in situ measurements.

***Index Terms***— Coherent X-band Radar, Nearshore wavefield observation

## 1. INTRODUCTION

The dissipation of the wave energy and the transformation of the wave field propagating over uneven bottom towards the shore has been subject of study for decades. Many experiments, at wave tanks and at the field, have been implemented since the 60's. At the experiment with the denser wave sensors array, [1] at DUCK, there were less than twenty sensors measuring wave height. By this it turned out that the monitoring of a shoaling wave field is still undersampled by using in situ measurements. Relatively recently this problem is countered by using ground based remote sensing techniques, e.g. from cameras, a review at [2] or from (coherent) radar systems [3] and [4].

Nevertheless, the application of coherent radar systems for the monitoring of the wave- and current- field at the nearshore has not extensively applied. The reason for the limited application is the impact of the complexity of the hydrodynamic phenomena on the backscattered electromagnetic waves. The acquired Doppler spectra (and out of them, the calculated Doppler velocities) reflect the locally dominant scattering mechanism, which is impacted by the instantaneous and local hydrodynamic conditions.

This paper presents for the first time, the monitoring of the wave field propagating the last nautical mile towards the coast by using a ground based Dopplerized X-band radar with horizontal polarization. The objective is the extraction of oceanographic information from the coherent signal by, firstly, interpreting the microwave scatterers in the littoral zone.

## 2. LITTERATURE REVIEW

The investigation of the interactions between the electromagnetic waves and the sea waves consist a major research subject, since the WW-II, for different and at the beginning non-civil applications. Crombie [5], by using a HF radar, published the first oceanographic results and he correlated the measured Doppler frequency with the phase velocity of the water waves. Concurrently and after him, with the development of variant radar systems (including most of the electromagnetic frequencies for different targets or for different carrier platforms) the scattering mechanism for radar returns to be investigated.

For the wind-wave surfaces which fall into the 'slightly rough' category moderate or high grazing angle the primary mechanism is the Bragg scattering, e.g. [6]. From direct measurements of Doppler spectra of any given wind-wave field, the mean speed of the Bragg-resonant water wave has been obtained [7], [8]. At the low grazing angles (LGA) the Bragg backscatter mechanism is not the dominant, but other mechanisms can be taking place simultaneously [9], [10]. The underlying hydrodynamic and atmospheric phenomena have significant impact on the measured Doppler velocity, which is the powerweighted mean of the phase velocity of both the advancing and receding scatterers (Bragg) resonant waves in a resolution cell plus any advection of the facet due to gravity wave orbital velocities, surface currents, and wind drift e.g. [3], [9], [11]-[12].

In addition to previously mentioned phenomena, in the littoral zone the waves release their energy by breaking. The breakers, and the LGA, intensify the non-Bragg backscattering mechanisms. It has been observed that the backscatter of the wave breakers or phenomena generated by the breakers have large radar cross section values (sea spikes) and Doppler velocities on the order of a few m/s, among several studies: [9] [13]- [14]. The importance of the wave steepness and surface roughness at low grazing angles has been discussed by several [15]-[17]. Analysis of field data collected in the ocean covering wind speeds from 7 to 15 m/s, grazing angles from 1.4° to 5.5°, and with different levels of background swell influence resulted that the breaking effects are increasing significantly the Doppler velocity of both polarizations (about 50% faster) and enhancing the horizontally polarized backscattering cross-section drastically (with 10-15 dB increase) [17].

This short literature review of the backscatter mechanism in relation of the hydrodynamics demonstrates the complex relationship that exists between microwave backscatter and nearshore processes. This relationship is explored here by characterizing microwave scattering in the nearshore and relating the measurements to nearshore waves and water surface velocities.

## 3. EXPERIMENT

The area of research is located at the north-west side of the Sylt Island, laying in the German Bight. The coast is an exposed

littoral sandy dune and characterized as mixed energy-tide dare; the tide is semi-diurnal and the tidal range reaches approximately 2 m, which causes cross shore transport through the channels between the barrier islands. The long shore transport along the coast is mainly wave induced. The maximum depth of the area covered by radar, is 8 m and there is a sand bar parallel to the coast, between the isolines of 3m and 4 m

The instrumental setup of the experiment includes a dopplerized marine radar system horizontally polarized, a meteorological station, 2 wave riders and 2 tide gauges. The radar was developed on the base of nautical X-band ($\lambda_{radar} = 3cm$) radar [18]. The main modification is the coherentisation of the transmitter - receiver module to detect the Doppler frequency shifts in 254 range cells, with spatial resolution of 7.5 m. The resulting range is 1920 m, along a radial beam and the temporal length of the observation is 10 min, the sampling frequency is 1024 pulses per second.

During the experiment, all the measurements were synchronous and the data were transmitted to the field operational center in real time. The wind conditions vary between 4-9Bft and by knowing the actual wave conditions from the wave riders, the radar was steered against the direction of the wave propagation. Thus, the wavefield was monitored perpendicular and the effect of the current field on the wavefield was minimized.

## 4. DATA PROCESSING

The complex valued data are separated into chunks of 512 successive radar pulses, corresponding approximately to 0.5s; each of them is considered as one sample and fast Fourier transformation is applied on it. The frequency resolution of the resulting spectra is $\Delta f = 1.95\,\mathrm{Hz}$ and the Nyquist frequency is $f_{max} = 512\,\mathrm{Hz}$. The radial velocity is calculated for each bin by the $v_{rad} = 0.5\lambda_{radar} f_{doppler} / \cos(\theta_g)$; $\theta_g$ is the grazing angle and $v_{rad} = v_w + v_{orb} + v_{cur} + c_p$, where $v_w$, $v_{orb}$, $v_{cur}$, $c_p$ are the wind drift the orbital motion, the current velocity and c the velocity of the scatterer, respectively. The Nyquist frequency corresponds to the velocity of 7.5 m/s with a bin size of 2.9 cm/s. In this case, as the radar is shore-based and the waves are propagating towards the coast, the velocity of the wave crests imaged by the radar is only positive and the negative values correspond to aliased frequencies, therefore the Doppler spectra are unwrapped by simply moving the negative part to the upper end of the spectrum.

At the first step of data analysis the data are smoothed with moving average with span of 5 bins, which does not affect the statistical properties of the spectra. Next step, the signal to noise ratio is calculated for each frequency, in case that the ratio is lower than 1, the spectral density was set equal to 0, Fig. 1. Based on the peak position of the spectrum, the Doppler velocities were calculated; the result is geocoded.

Due to the instruments properties, the backscattering mechanism at the low grazing angle and the shadowing, in the time series of the row data, there are gaps in the recorded signal, the amplitude is equal to zero, therefore higher harmonics exist in the resulted spectra, which outflank the frequency of the backscattered signal. To filter out the ambiguous velocities, two different methods were followed. At the first one, the number of naught signal values into each time chunk was counted and the chunks with more than 15% missing values were excluded.

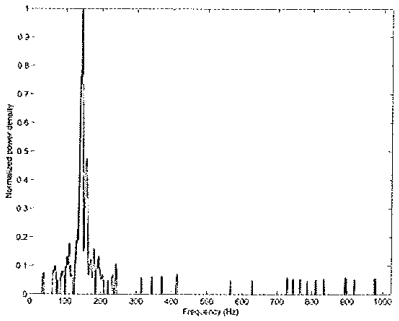


Figure. 1. Normalized Doppler spectrum after the smoothing and the subtraction of the noise.

For the second approach, the moments of the Doppler spectra were calculated, based on them, the width of the spectra was evaluated. Among the width indicators of the Doppler spectra utilized for evaluating the signal quality, the $qp = 2\Sigma f^2 S_D / (\Sigma S_D)^2$ was the most robust, where $S_D$ is the Doppler spectrum, the threshold is set 0.3. At fig. 2, the relation of the two quantities with the Doppler velocities is illustrated.

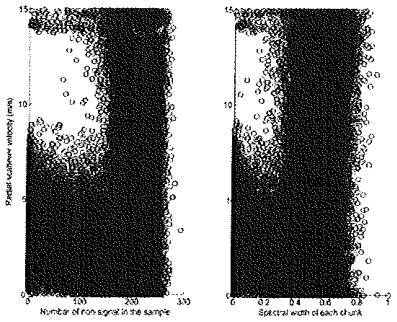


Figure. 2. The scatterplots of the number of missing values in the data (critical value 120) and of criterion qp for the spectral width (critical value 0.35) as function of the Doppler velocity.

The performance of the two different methods is similar and the influence of shadowing is increased with the distance from the radar; therefore the number of available data is reduced Fig. 3.

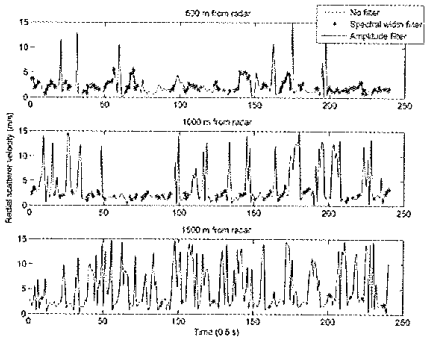


Figure. 3. Three 2-min interval of consecutive 0.52-s radial scatterer velocity estimates computed by tracking the peak of the each Doppler spectrum (the green line), the red stars and the blue line are the velocities filtered in by the spectral width (red stars) and the existence of values (blue line).

## 5. RESULTS AND DISCUSSION

The product of the analysis is a set of 200 simultaneous time series of the horizontal velocity of the scatterers on water surface in the coastal zone, with spatial resolution of 7.5 m, Fig. 4; thus time series of 10 min with gaps due to the filtering were created. The number of the available measurements is reduced with the range, dark blue at Fig. 4. The parallel lines of the velocities, demonstrate that the scatterers travel towards the shore on top of the long waves.

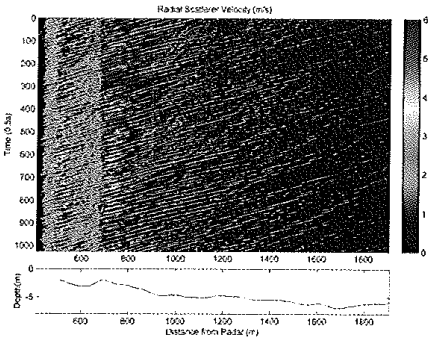


Figure 4. Top: Range – time image of filtered horizontal velocity extracted from the radar. Bottom: The cross-section of the bathymetry under the radar beam.

In addition the impact of the bathymetry is obvious, at the isobath of 2 m, where lying the first sand reef, the waves break and the velocity of the scatterers is almost the double, after the reef towards shore, the velocity is reduced and again is increased on the second sand bar; the same features are observed also to the average over time. In both cases the factor of the velocity boost is approximately 1.5 – 2 in comparison with the non-breaking zone, Fig. 5.

The average in time of the without filtering Doppler velocities, which include the low amplitude values, is extremely high, the order of which has a factor of 2 in comparison with the filtered velocities. In all the three cases the effect of shadowing in range is obvious. The shadows are introduced in high frequencies, which has a threshold behavior for their detection.

By considering that the scattering-object velocity in the water frame of reference obtained from the Doppler frequency, is the sum of the wind drift of the current velocity including the orbital motion and the speed of the scattering object, in the following paragraphs, the measured radial velocities are evaluated. For the evaluation, the range bins between 900 m and 1000m from the radar, are used, because the area has constant depth and there are fewer gaps in the time series of the Doppler velocity in comparison with the time series further from the radar.

During the data acquisition, the mean measured wind velocity at 10 m height on the coast was 17.3 m/s. The approximation of the calculation of the wind drift is 2.5 -5.1% of the wind speed, [19]. Under the assumption that the wind field is homogeneous and due to the high wind velocity, the wind drift is calculated as the 4.3% of the wind speed [20]. Therefore, the input of the wind in the Doppler velocities is in the range of $v_w = 0.73$ m/s.

In addition, the significant wave height at the nearest wave rider, at depth of 6m was measured 1.5 m with wave period 10 s. By applying the linear wave theory, the horizontal component of the orbital velocity is calculated $v_{orb} = 1.1$ m/s.

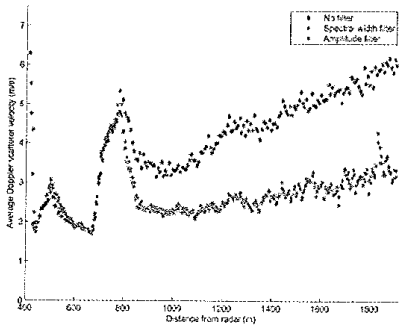


Figure 5. Average Doppler spectral velocities, before the filtering (blue) and after (spectral width and amplitude, red and green respectively) in time for the whole range of the radar beam.

The measurement was acquired one hour before high water; a typical value of the current velocity for this area during low wind conditions is $v_{cur} = 0.2 - 0.4$ m/s. To avoid the measurement of the Doppler shift due to the currents, the radar was steered in the propagation direction of the wavefield, but probably this data acquisition strategy has limited effectiveness during stormy conditions in the coastal area, where rip and longshore currents are generated.

By summing up, the velocities of the individual hydrodynamic phenomena and subtracting the sum from the Doppler radial

velocity, the velocity of the scatterer $c_p$ was calculated for the subarea of interest in the order of 0.3 m/s.

## 6. CONCLUSIONS

This first investigation in the coastal zone, based on a horizontally Dopplerized radar system proved that the Doppler velocity of the sea surface could quantify the ongoing processes under specific assumptions, during stormy conditions.

Due to the low grazing angle and the interference of the electromagnetic waves with the sea surface, the recorded backscatter signal has missing values. To encounter this problem, two different approaches have been applied; the first one in the time domain and the second in the frequency domain. Both of them perform the same and increase significantly the applicability of the data for geophysical observations.

From the geophysical point of view, the mean velocity of the scatterers related to the sea surface is measured for the last 2 km approaching the shore. For the homogeneous area, in a distance of 1000 m from the radar, where the remaining values are enough, the measured velocity is validated and it seems to be reasonable in comparison with the hydrodynamic environmental conditions. The radial velocity is influenced by the bathymetrical variations; more specific at the breaking zone the radial speed is twice higher than in the homogenous areas.

Further and current investigations focus on the application of non-uniform fast Fourier transformation due to the gaps, the determination of the Doppler frequency with more robust methods, e.g. the moments, and the establishment of a transfer function for the extraction of the spectral wavefield properties from the spectra of the radial velocities.

## 7. REFERENCES


[1] T.H.C. Herbers, S. Elgar, R.T.Guza, and W.C. O'Reilly, "Surface gravity waves and nearshore circulation," DUCK94 Experiment Data Server: SPUV Pressure Sensor Wave Height Data. 2006.

[2] H.F. Stockdon, and R.A. Holman, "Estimation of wave phase speed and nearshore bathymetry from video imagery," Journal of Geophysical Research 105, pp. 22015–22033, 2000.

[3] S.J. Frasier, Y. Liu, D. Moller, R.E. McIntosh and C. Long, "Imaging Radar Directional Ocean Wave Measurements in a Coastal Setting Using a Focused Array," *IEEE TGRS*, 33, 2, 1995.

[4] J. A. McGregor, E. M. Poulter, and M. J. Smith, "S band Doppler radar measurements of bathymetry, wave energy fluxes, and dissipation across an offshore bar," *J. Geophys. Res.*, vol. 103, 1998.

[5] D. D. Crombie, "Doppler spectrul at Sea Echo at 13.56 Mc/s," *Nature*, p. 2, April 16 1955. [9]

[6] J. Wright, "A new model for sea clutter," *Antennas and Propagation, IEEE Transactions on*, vol. 16, pp. 217-223, 1968.

[7] V. W. Pidgeon, "Doppler Dependence of Radar Sea Return," *J. Geophys. Res.*, vol. 73, 1968.

[8] J. R. Duncan, W. C. Keller, and J. W. Wright, "Fetch and wind speed dependence of Doppler spectra," *Radio Sci.*, vol. 9, 1974.

[9] P. H. Y. Lee, J. D. Barter, K. L. Beach, C. L. Hindman, B. M. Lake, H. Rungaldier, J. C. Shelton, A. B. Williams, R. Yee, and H. C. Yuen, "X band microwave backscattering from ocean waves," *J. Geophys. Res.*, vol. 100, 1995.

[10] J. Morris, S. Anderson, and S. Cloude, A study of the X-band entropy of breaking ocean waves, in *IEEE International Geoscience and Remote Sensing Symposium, 2003. IGARSS '03*, vol. 2, 2003

[11] G. Farquharson, S. J. Frasier, B. Raubenheimer, and S. Elgar, "Microwave radar cross sections and Doppler velocities measured in the surf zone," *J. Geophys. Res.*, vol. 110, 12/23 2005.

[12] W. J. Plant and W. C. Keller, "Evidence of Bragg Scattering in Microwave Doppler Spectra of Sea Return," *J. Geophys. Res.*, vol. 95, 1990.

[13] B. L. Lewis and I. D. Olin, "Experimental study and theoretical model of high-resolution radar backscatter from the sea," *Radio Sci.*, vol. 15, 1980.

[14] Y. Liu, S. J. Frasier, and R. E. McIntosh, "Measurement and classification of low-grazing-angle radar sea spikes," *Antennas and Propagation, IEEE Transactions on*, vol. 46, pp. 27-40, 1998.

[15] W. J. Plant, W. C. Keller, V. Hesany, T. Hara, E. Bock, and M. A. Donelan, "Bound waves and Bragg scattering in a wind-wave tank," *J. Geophys. Res.*, vol. 104, 1999.

[16] P. H. Y. Lee, J. D. Barter, K. L. Beach, B. M. Lake, H. Rungaldier, H. R. Thompson, Jr., L. Wang, and R. Yee, "What are the mechanisms for non-Bragg scattering from water wave surfaces?," *Radio Sci.*, vol. 34, 1999 1999.

[17] P. A. Hwang, M. A. Sletten, and J. V. Toporkov, "Analysis of radar sea return for breaking wave investigation," *J. Geophys. Res.*, vol. 113, 02/6 2008.

[18] N. Braun, F. Ziemer, A. Bezuglov, M. Cysewski, and G. Schymura, "Sea-Surface Current Features Observed by Doppler Radar," *Geoscience and Remote Sensing, IEEE Transactions on*, vol. 46, pp. 1125-1133, 2008.

[19] P. Lange and H. Inerfuss, "Drift Response of Monomolecular Slicks to Wave and Wind Action," *Journal of Physical Oceanography*, vol. 8, pp. 142-150, January 01, 1978 1978.

[20] G. Tomczak, "Investigations with drift cards to determine the influence of the wind on surface currents," *Tokyo Geophys. Inst. Stud. Oceanogr.*, vol. 10, pp. 129-139, 1964.